Pore-Scale Imaging of Solid Bitumens: Insights for Unconventional Reservoir Characterization*

Tim E. Ruble[1], Kultaransingh (Bobby) Hooghan[1], William Dorsey[1], Wayne R. Knowles[1], and Christopher D. Laughrey[2]

Search and Discovery Article #80580 (2017)**
Posted March 6, 2017

*Adapted from oral presentation given at AAPG Hedberg Research Conference, Santa Fe, New Mexico, October 16-19, 2016

[1]Weatherford International Ltd., Houston, TX, USA (tim.ruble@weatherfordlabs.com)
[2]Weatherford International Ltd., Evergreen, CO, USA

Abstract

Characterizing unconventional reservoirs involves the investigation of a wide range of potential source rock targets at various stages of thermal maturity. These samples may contain a mixture of kerogen, bitumen, oil and pyrobitumen within their fabric. Thus, it is critical that we properly identify and examine each organic phase in order to better understand reservoir properties. In the present study, we have selected samples of gilsonite from a naturally occurring solid hydrocarbon deposit to serve as an analog for characterizing the bitumen phase of generation.

Gilsonite is an aromatic-asphaltic solid bitumen that is found in vertical veins along the eastern portion of the Uinta Basin, Utah. It is thought to be an early generation product from oil-prone Green River Shale source beds and is similar to low maturity crude oil in composition. It has a high nitrogen content, low sulfur content, high melting point (fusibility) and is soluble in organic solvents. We have used a variety of analytic methods to characterize this material, including standard optical organic petrology and scanning electron microscopic imaging to examine the occurrence of organic porosity.

Optical organic petrology analysis using both air and oil immersion objectives show that the polished gilsonite surfaces are typically dark grey and featureless. Macerals and inorganics are absent. Visual estimates suggest that fractures make up approximately 1% of the conchoidal fracture plane, while the pencillated variety contains approximately 2% fractures along with 5% shallow pits. Scanning electron microscopic images also show the occurrence of fractures within gilsonite, but the matrix contains no evident organic porosity.

The results of our analyses suggest that, unlike pyrobitumen, pre-oil solid bitumen represented by gilsonite was found to contain no significant occurrences of organic nanoporosity within its matrix. Gilsonite does have minor pitting and fractures, but these do not represent an effective interconnected pore network and are probably artifacts of weathering/sampling. Thus, this material would not represent a potential candidate for in-situ hydrocarbon storage capacity. Whether this is typical of all naturally occurring solid bitumen is debatable, considering that gilsonite

has undergone some secondary alteration via devolatilization and limited biodegradation. Nevertheless, the pore-scale imaging of this solid bitumen provides potentially important new insights for unconventional reservoir characterization.

References Cited

Boden, T., and B.T. Tripp, B.T., 2012, Gilsonite veins of the Uinta Basin, Utah: Utah Geological Survey, Special Study 141, CD-ROM publication, 50 p., 1 pl.

Curiale, J.A., 1986, Origin of solid bitumens, with emphasis on biological marker results: in Leythaeuser, D. and Rullkötter, J., eds., Advances in Organic Geochemistry 1985, Pergamon Press, New York, p. 559-580.

Eldridge, G.H., 1901, The asphalt and bituminous rock deposits of the United States: in 22nd Annual Report of the U.S. Geological Survey, 1900-1901, Government Printing Office, Washington D.C., v. 22, pt. 1, p. 209-452.

Helms, J.R., X. Kong, E. Salmon, P.G. Hatcher, K. Schmidt-Rohr, and J. Mao, 2012, Structural characterization of gilsonite bitumen by advanced nuclear magnetic resonance spectroscopy and ultrahigh resolution mass spectrometry revealing pyrrolic and aromatic rings substituted with aliphatic chains: Organic Geochemistry, v. 44, p. 21-36.

Hunt, J.M., 1963, Composition and origin of the Uinta Basin bitumens: in Crawford, A.L., ed., Oil and Gas Possibilities of Utah, Re-evaluated, Utah Geological and Mineralogical Survey, Bulletin 54, paper 24, Utah Geological Society, Salt Lake City, p. 249-273.

Hunt, J.M., 1979, Petroleum geochemistry and geology: W. H. Freeman and Company, San Francisco, 617 p.

Lewan, M.D., 1987, Petrographic study of primary petroleum migration in the Woodford Shale and related rock units: in Doligez, B., ed., Migration of Hydrocarbons in Sedimentary Basins, Editions Technip, Paris, p. 113-130.

Lewan, M.D., 2011, Petroleum formation research through hydrous pyrolysis: Weatherford Laboratories Presentation, June 17, 2011.

Ruble, T.E., M.D. Lewan, and R.P. Philp, 2001, New insights on the Green River petroleum system in the Uinta basin from hydrous pyrolysis experiments: AAPG Bulletin, v. 85/8, p. 1333-1371.

Weatherford®
LABORATORIES

PORE-SCALE IMAGING OF SOLID BITUMENS: INSIGHTS FOR UNCONVENTIONAL RESERVOIR CHARACTERIZATION

Tim E. Ruble[1], Kultaransingh (Bobby) Hooghan[1], William Dorsey[1], Wayne R. Knowles[1] and Christopher D. Laughrey[2]

[1] Weatherford International Ltd., Houston, TX
[2] Weatherford International Ltd., Evergreen, CO

Investigation of Gilsonite may aid our understanding of Unconventional Oil Systems

- Better understand the nature and occurrence of bitumen.
- Develop testing methods to distinguish movable oil versus immobile bitumen.
- Use SEM imaging to examine the occurrence of organic porosity within bitumen.
- Understand role of water emulsions in bitumen occurrence and mobility.

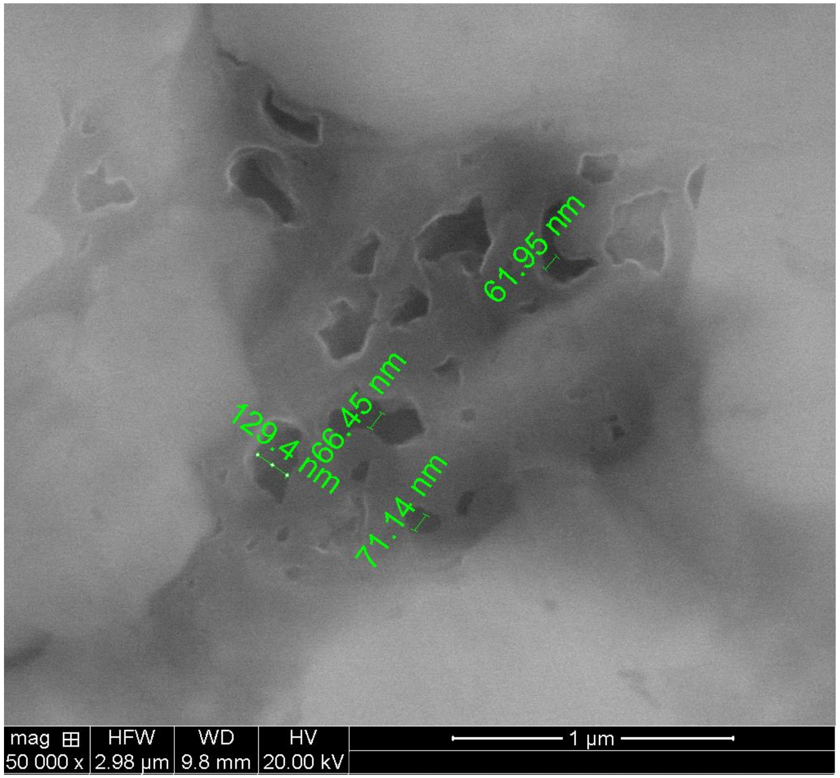

PYROBITUMEN HAS NANOPORES……WHAT ABOUT BITUMEN?

Weatherford® LABORATORIES

Hydrocarbon Generation

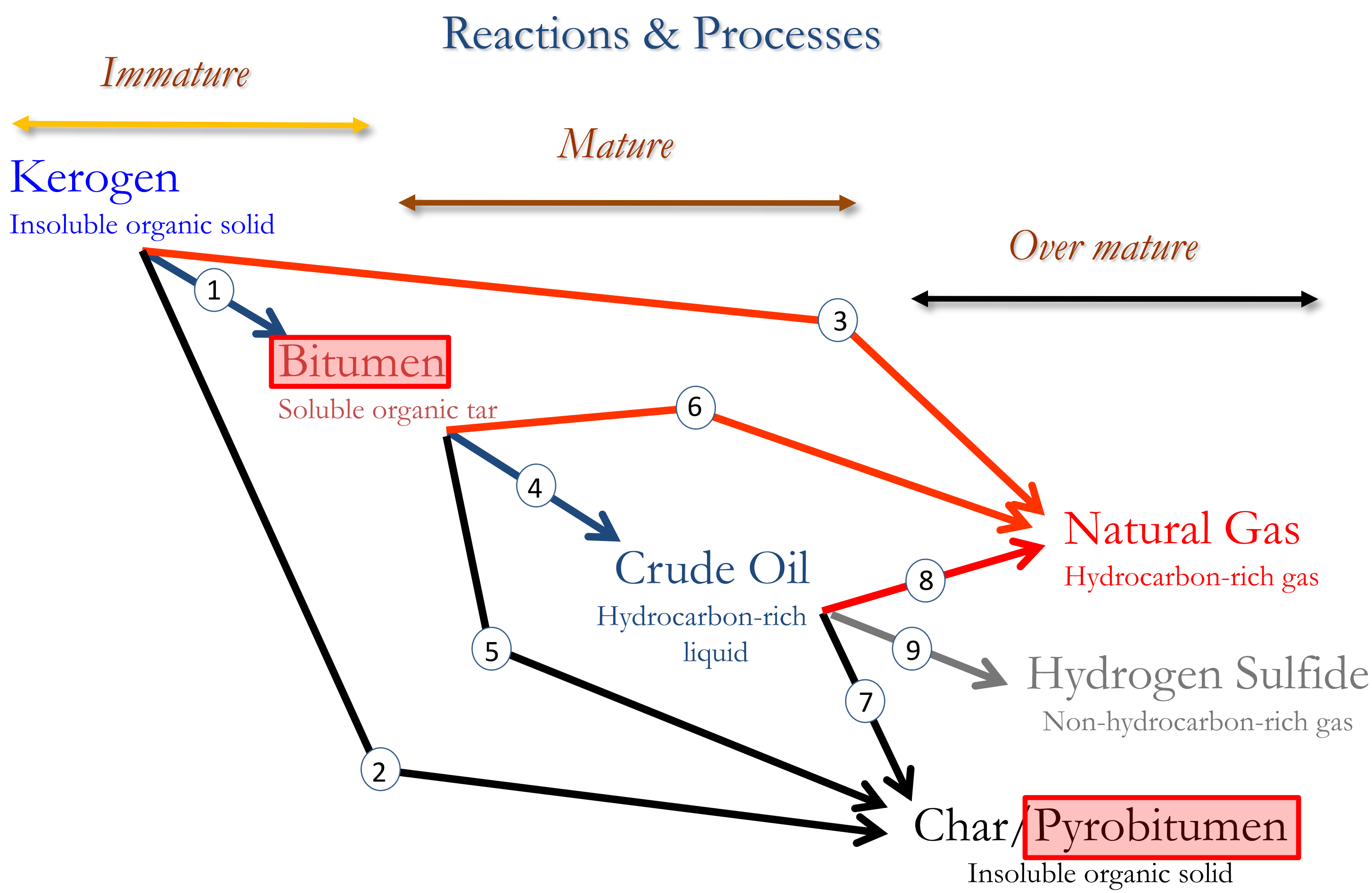

from Lewan (2011)

Weatherford LABORATORIES

Why is it important to distinguish "oil" from "bitumen"?

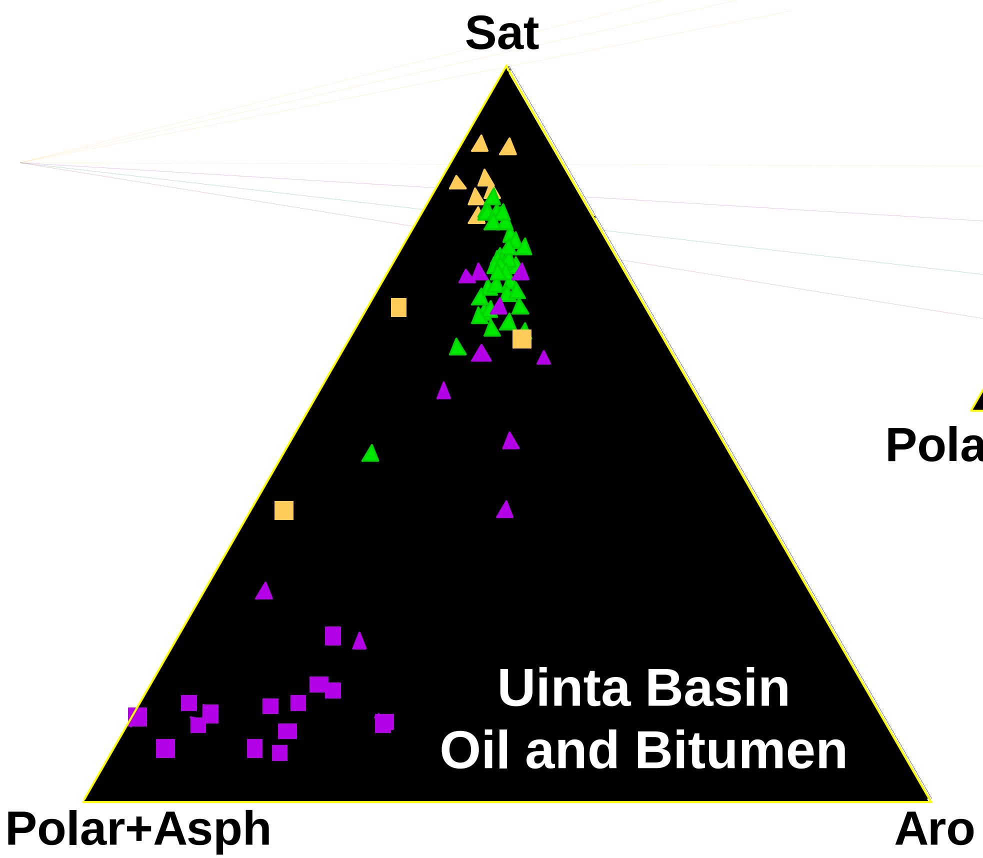

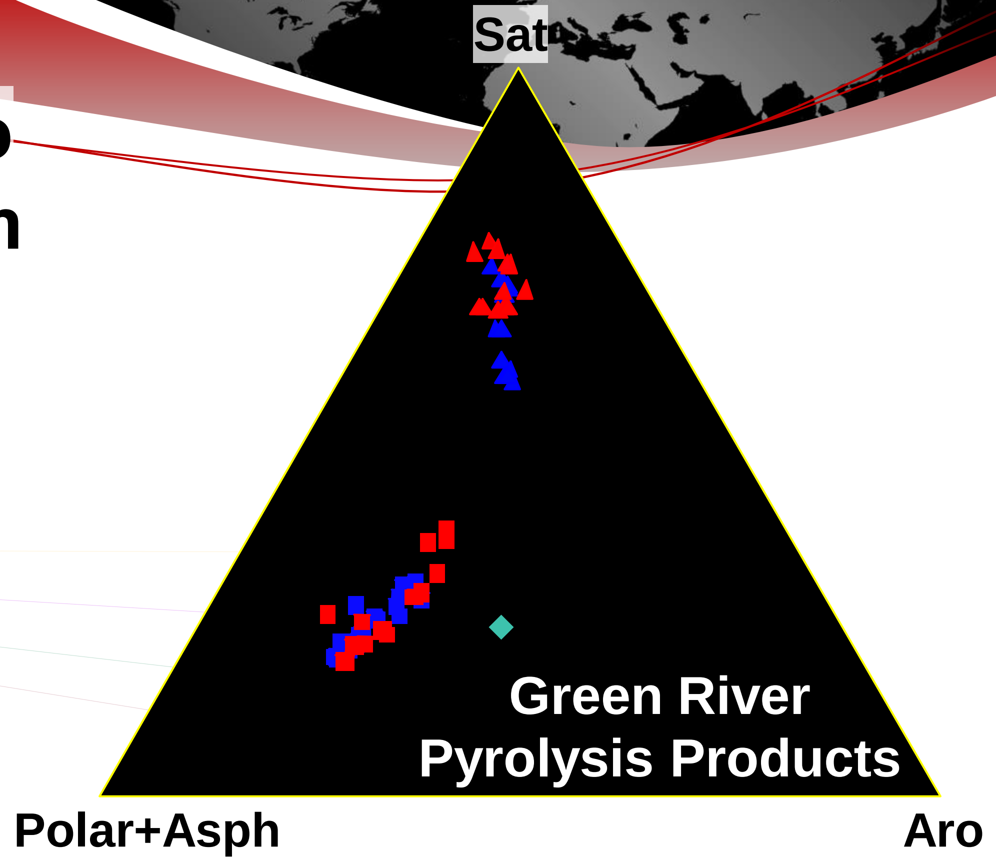

Because nature does!

from Ruble et al. (2001)

Weatherford LABORATORIES

Primary petroleum migration

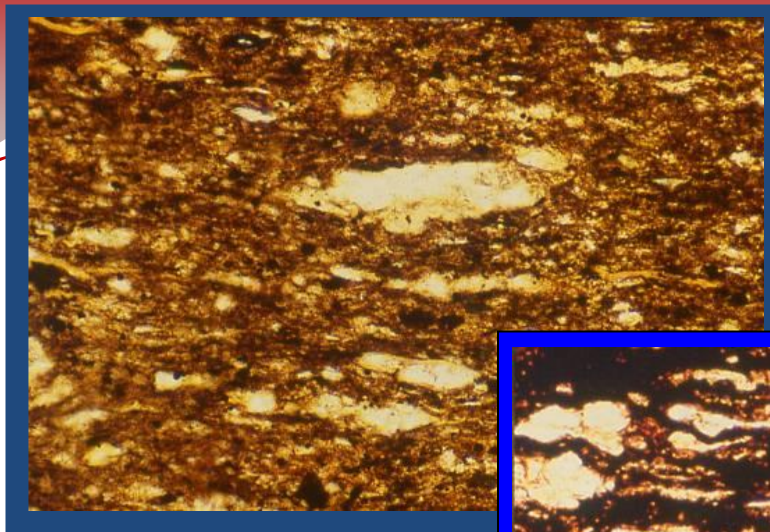

immature unheated

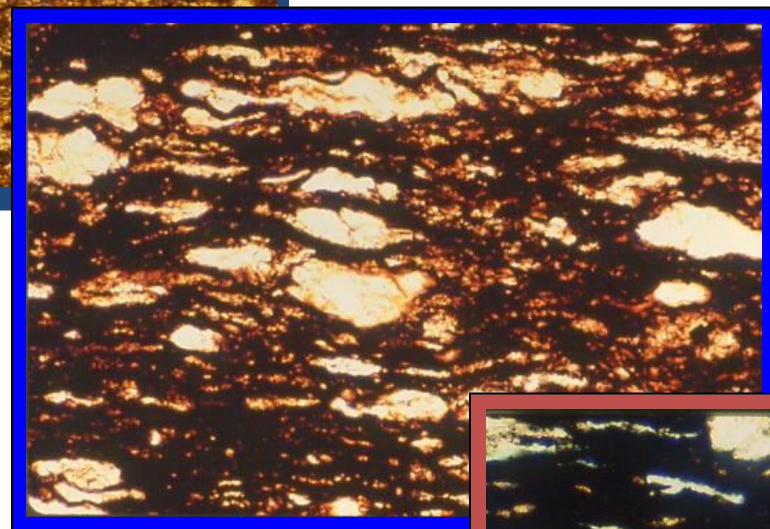

kerogen-bitumen
300°C/72h

125 µm

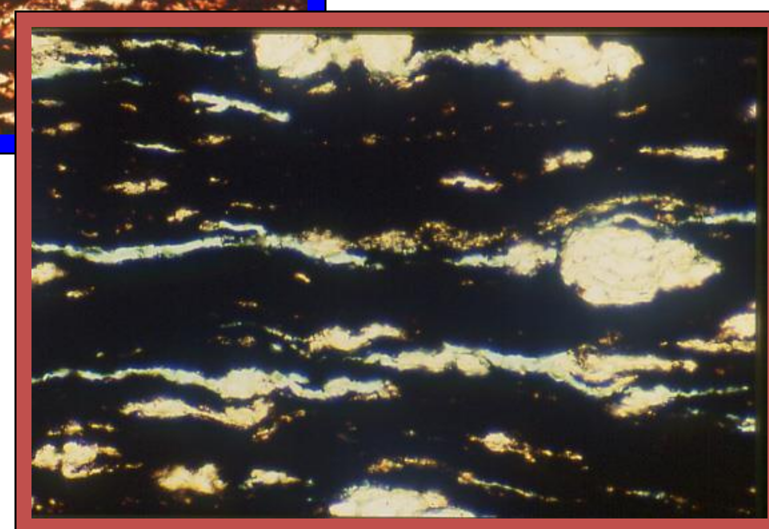

bitumen-oil 352°C/72h

Hydrous Pyrolysis of Woodford Shale Cores

from Lewan (1987)

Weatherford LABORATORIES

Generic Classification Scheme for Bitumens

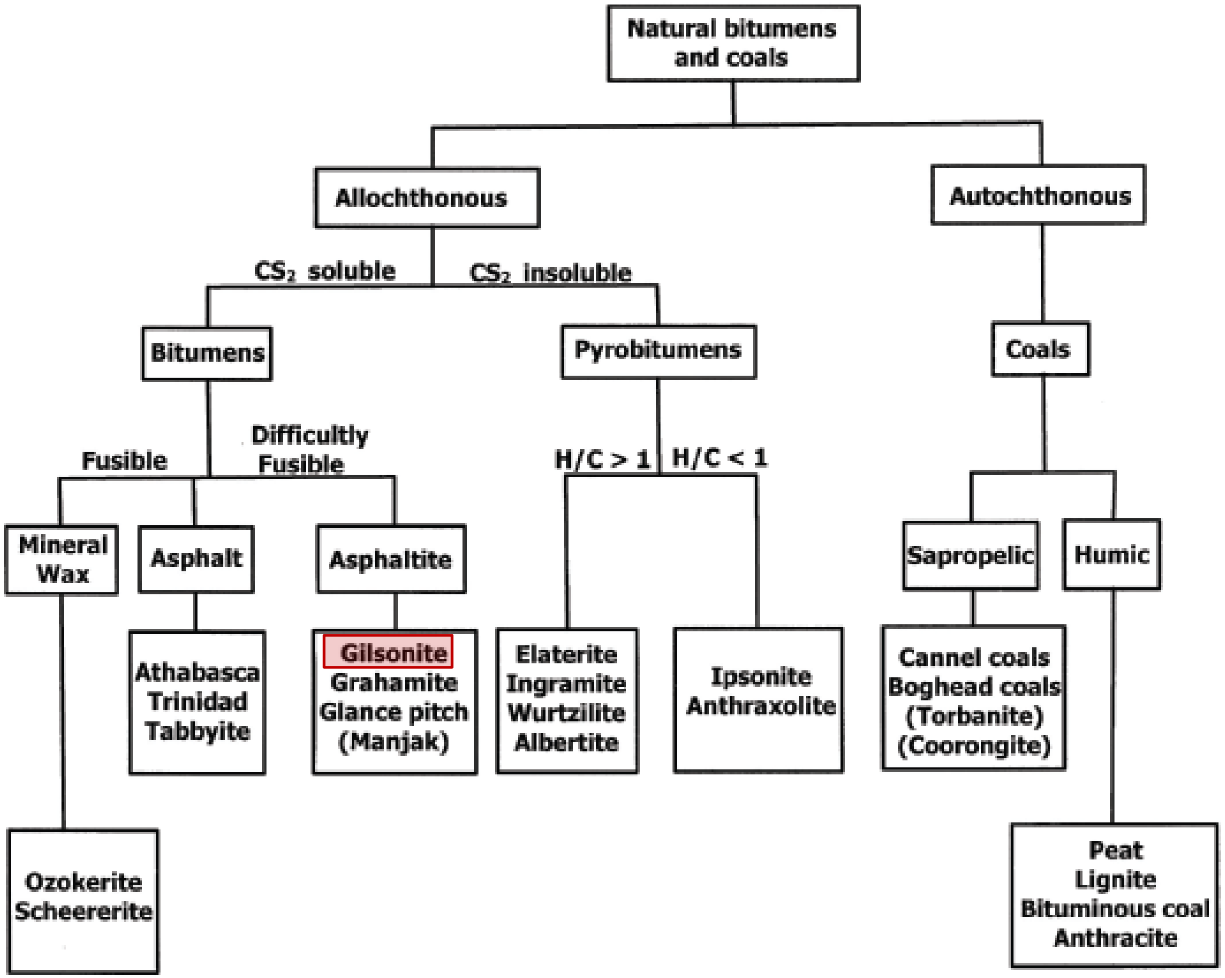

from Hunt (1979)

Weatherford®
LABORATORIES

Genetic Classification Scheme for Bitumens

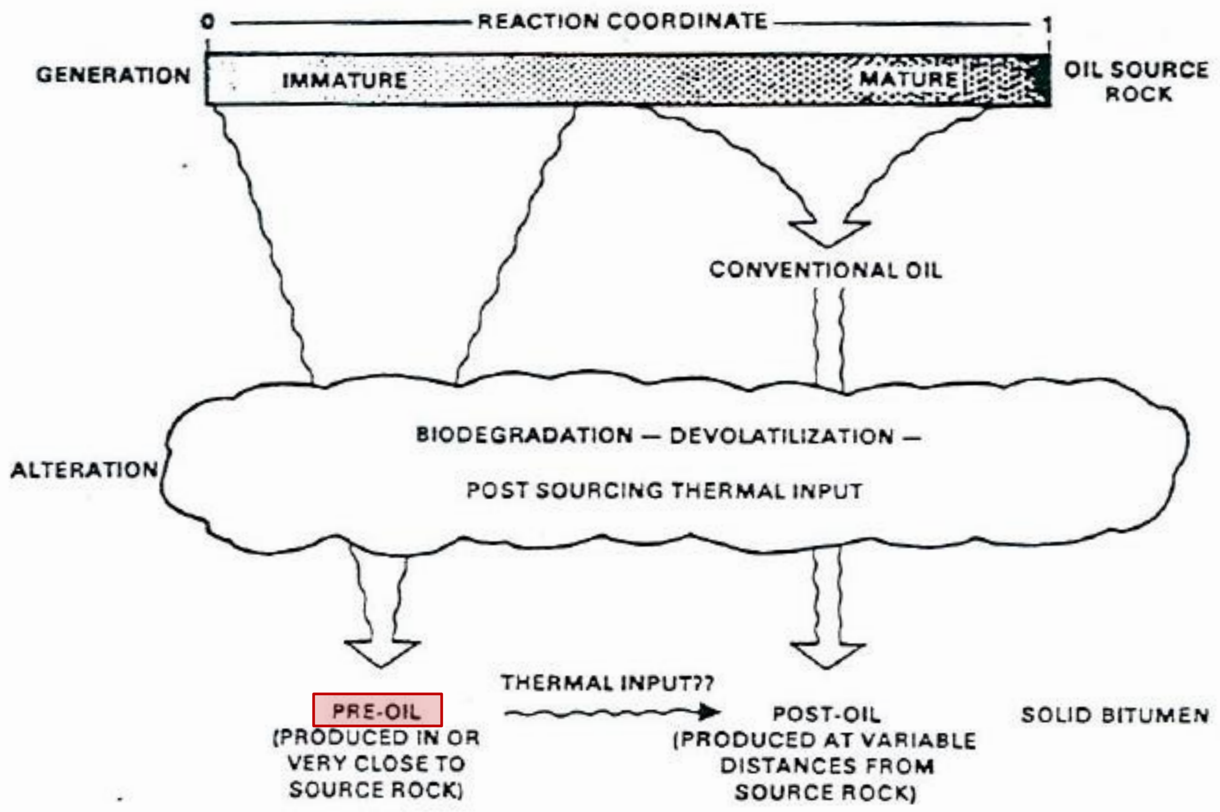

from Curiale (1986)

Weatherford LABORATORIES

Gilsonite Characteristics

- Solid to semi-solid
- Occurs in dikes or veins
  - Up to 5m x 40km
- Similar to low maturity crude oil in composition
- Aromatic-asphaltic hydrocarbons
- High nitrogen, low sulfur content
- Soluble in organic solvents (CS_2)
- High melting point (fusibility)

Weatherford® LABORATORIES

Gilsonite Textures

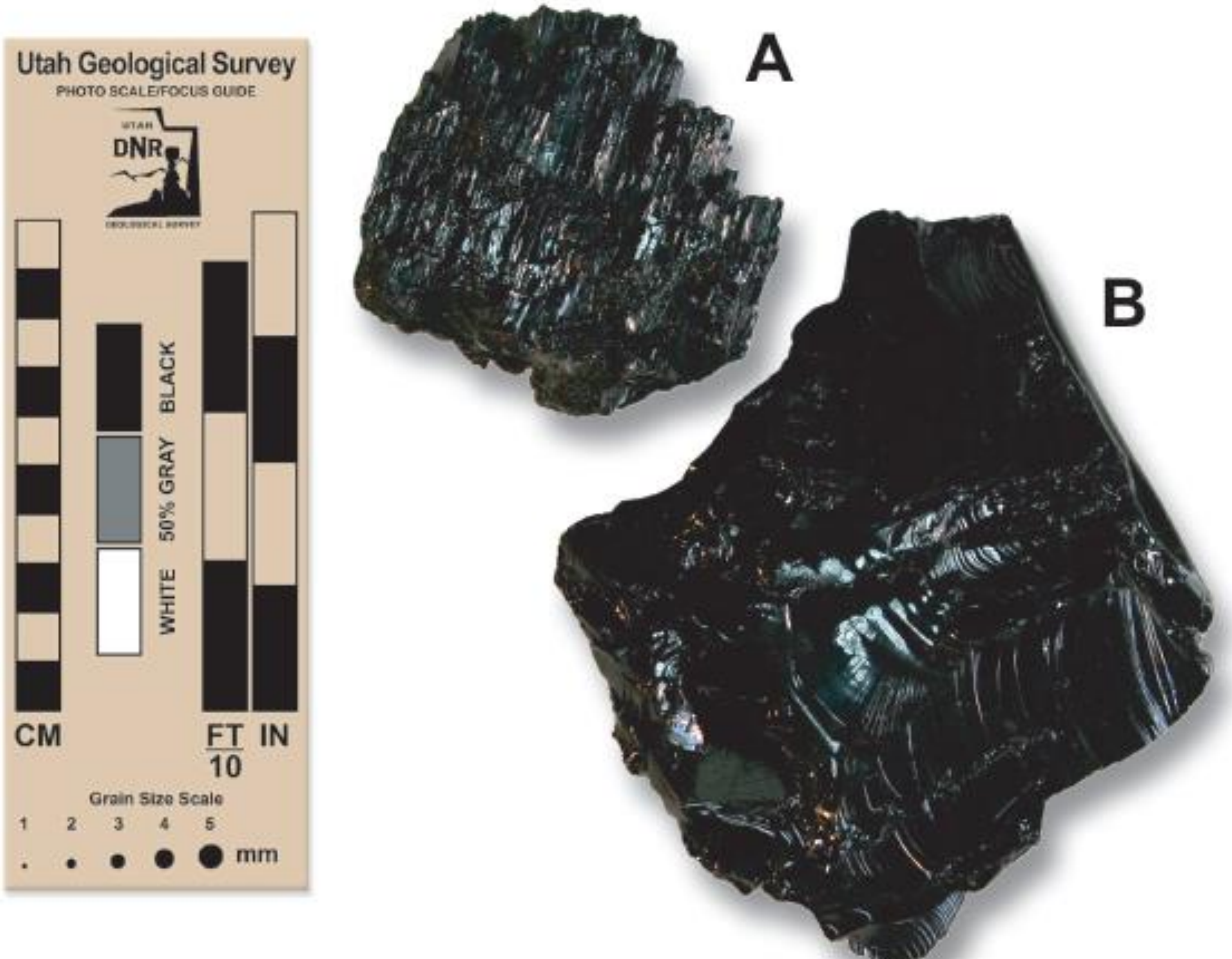

A) Gilsonite showing columnar “pencillated” structure

B) Gilsonite select grade showing “conchoidal” fracturing

from Boden & Tripp (2012) UGS Special Study 141

Weatherford® LABORATORIES

Uinta Basin Solid Hydrocarbon Deposits

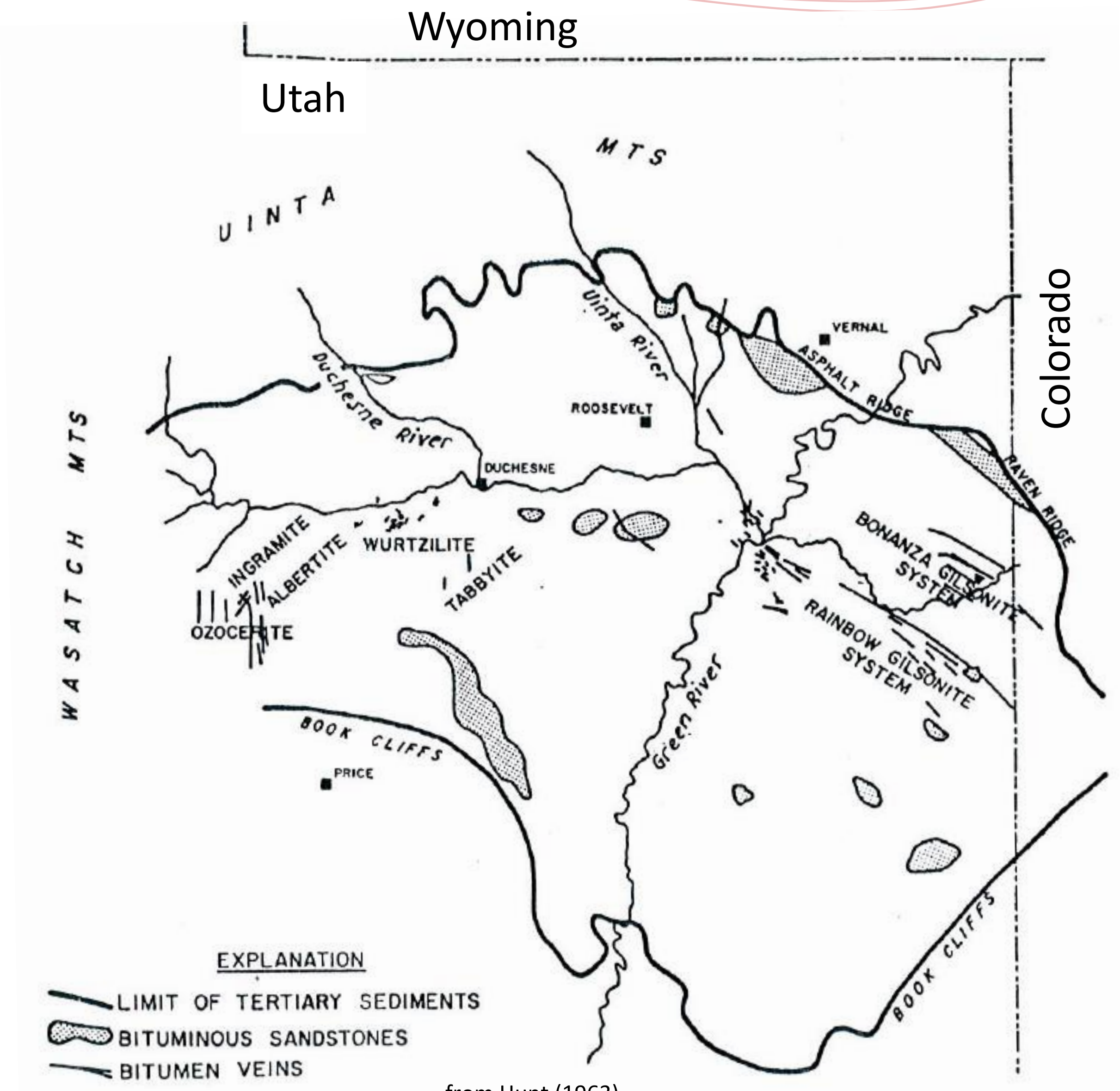

from Hunt (1963)

Gilsonite Veins

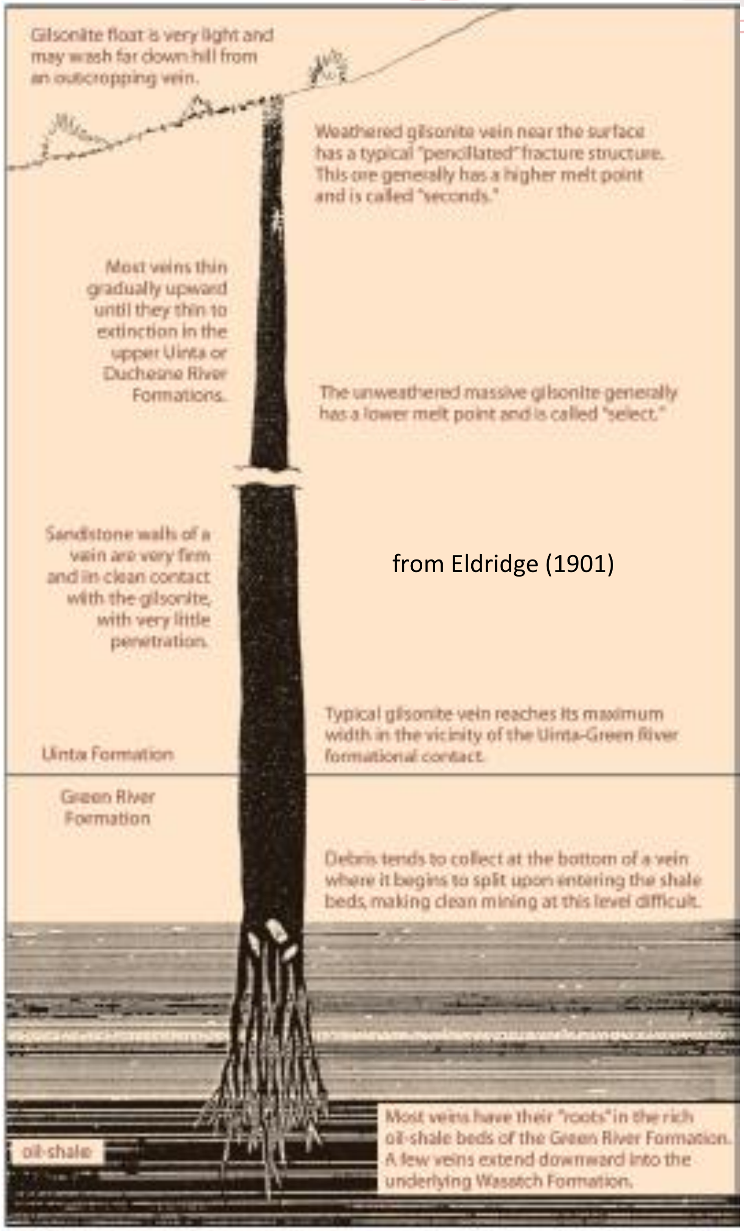

from Eldridge (1901)

Weatherford LABORATORIES

Gilsonite Tar - a mobile bitumen phase

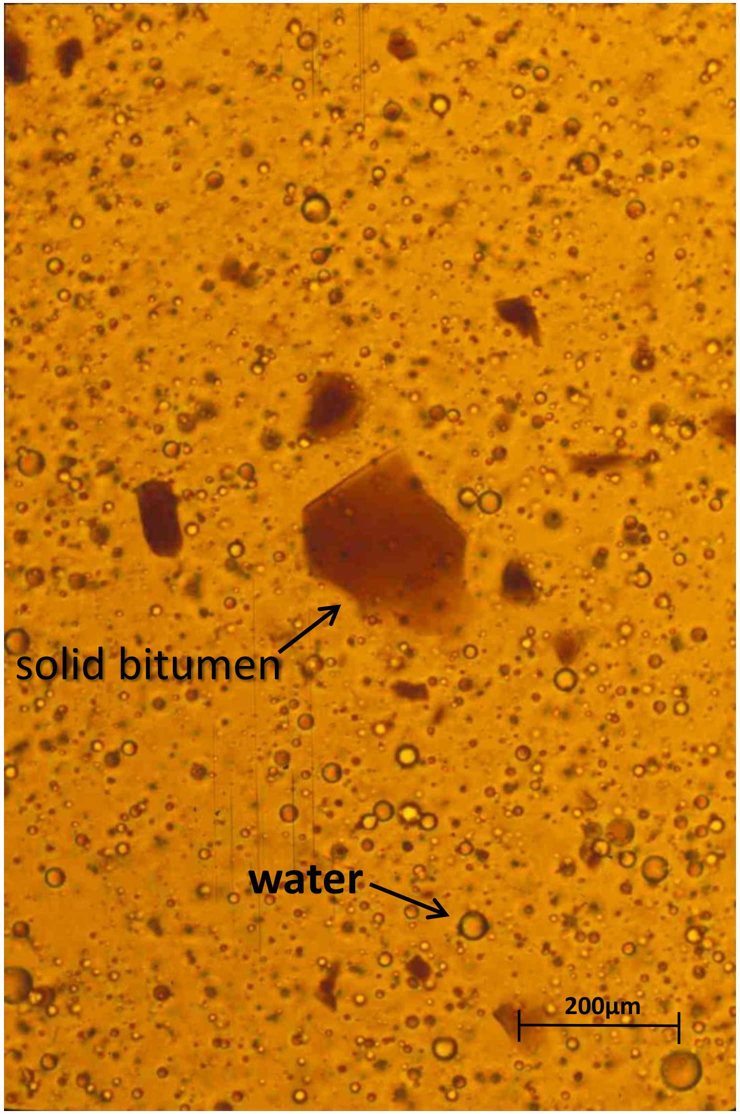

Viscous
Water in Bitumen/Oil Emulsion

Actively seeping into excavated gilsonite veins

Gilsonite precursor prior to solidification

Weatherford LABORATORIES

Origin of Gilsonite

1. Lacustrine oil shale kerogen →bitumen
   - Low thermal stress
   - Pre-oil generation stage

2. Expulsion from shale source rock – exceeds retention capacity – creates hydraulic fractures through extensive stress, viscous bitumen migrated vertically through fractures

3. Secondary alteration after injection into veins
   Solidification, devolatilization, possible biodegradation
   →Solid Bitumen

Weatherford LABORATORIES

Gilsonite Chemical Structure Model

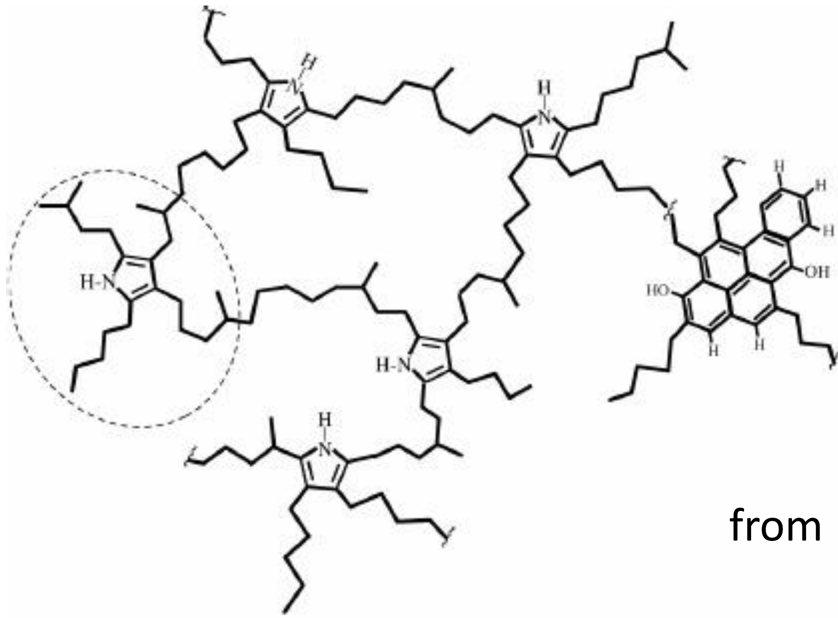

from Helms et al. (2012)

Model of the main components of gilsonite structure. A typical ‘‘monomer unit’’ containing one pyrrolic aromatic ring and 21 carbons is outlined by the dashed ellipse.

Gilsonite exists as a highly diverse mixture of molecules of various size and structure. The model structure shown here represents the high molecular weight fraction, while smaller fragments are also common.

Weatherford® LABORATORIES

Gilsonite Elemental Analyses

	Elemental analysis[a]	Solid state NMR	ESI-FT-ICR-MS number weighted	ESI-FT-ICR-MS intensity weighted
[a]Carbon wt%	80 (84.0)	83%	79.61	80.10
[a]Hydrogen wt%	(10.67)	11%	10.57	11.15
[a]Nitrogen wt%	3.3 (2.40)	≥3%	3.11	3.25
[a]Sulfur wt%	(0.50)	N/A	0.88	1.04
[a]Oxygen wt%	(3.74)	3.2%	5.83	4.32
[a]H/C atomic ratio	(1.51)	1.49	1.59	1.67

[a] Values in parentheses are averages based on literature values (Bell and Hunt, 1963; Clark et al., 1983; Jacob, 1989).

from Helms et al. (2012)

Weatherford LABORATORIES

Gilsonite EDS Spectra

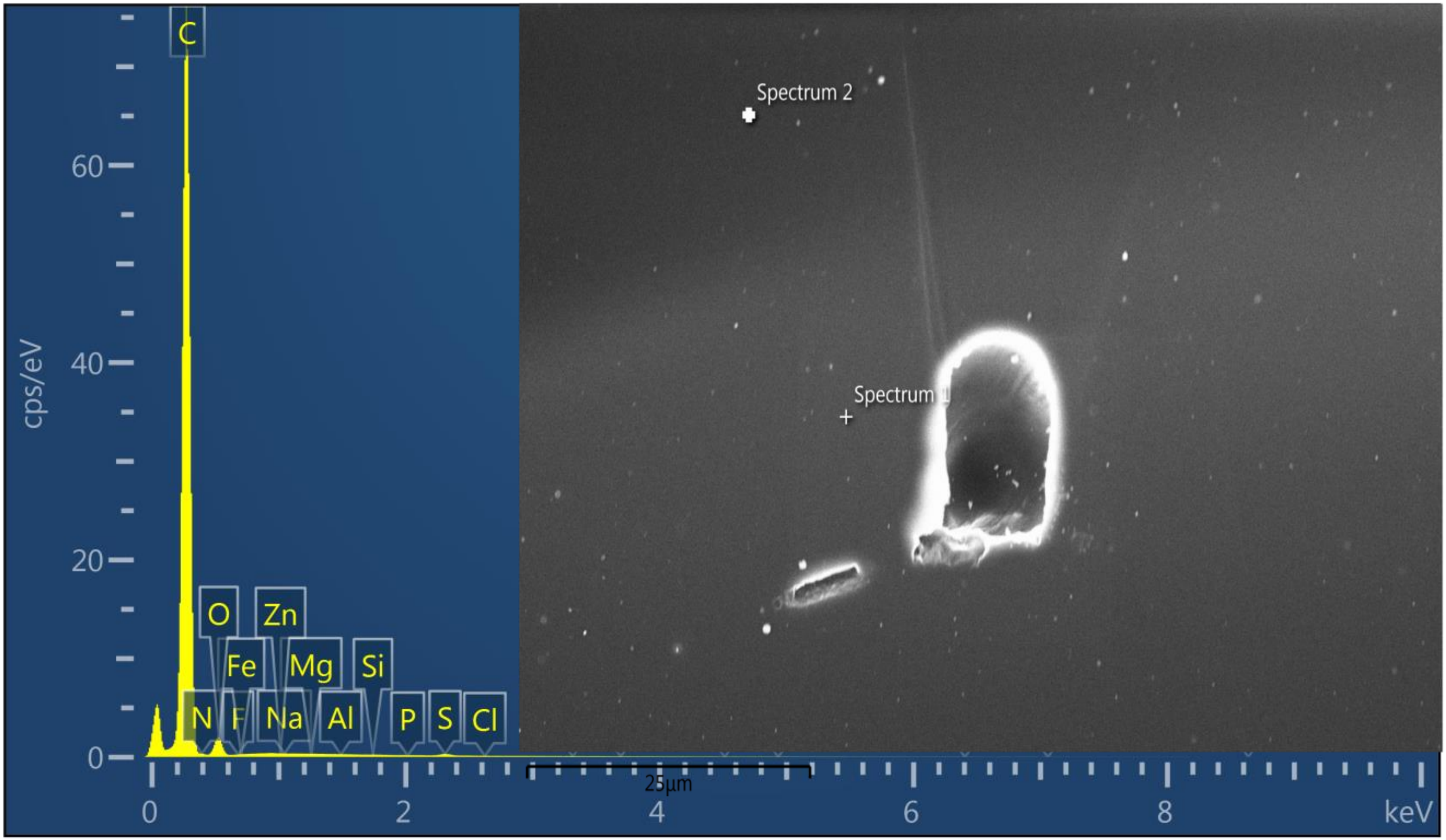

Weatherford®
LABORATORIES

Gilsonite EDS Elemental Maps

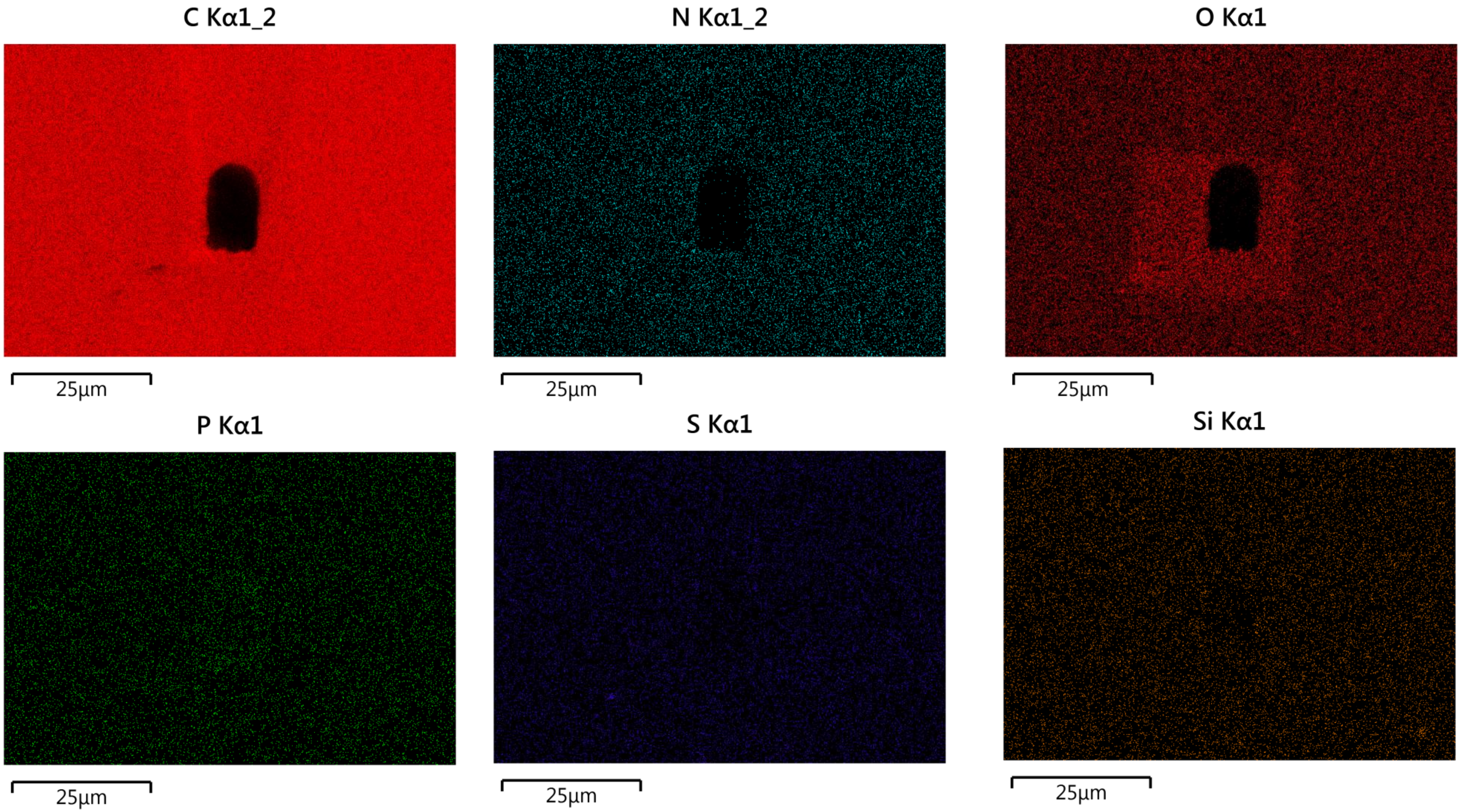

Weatherford®
LABORATORIES

Scale of Characterization

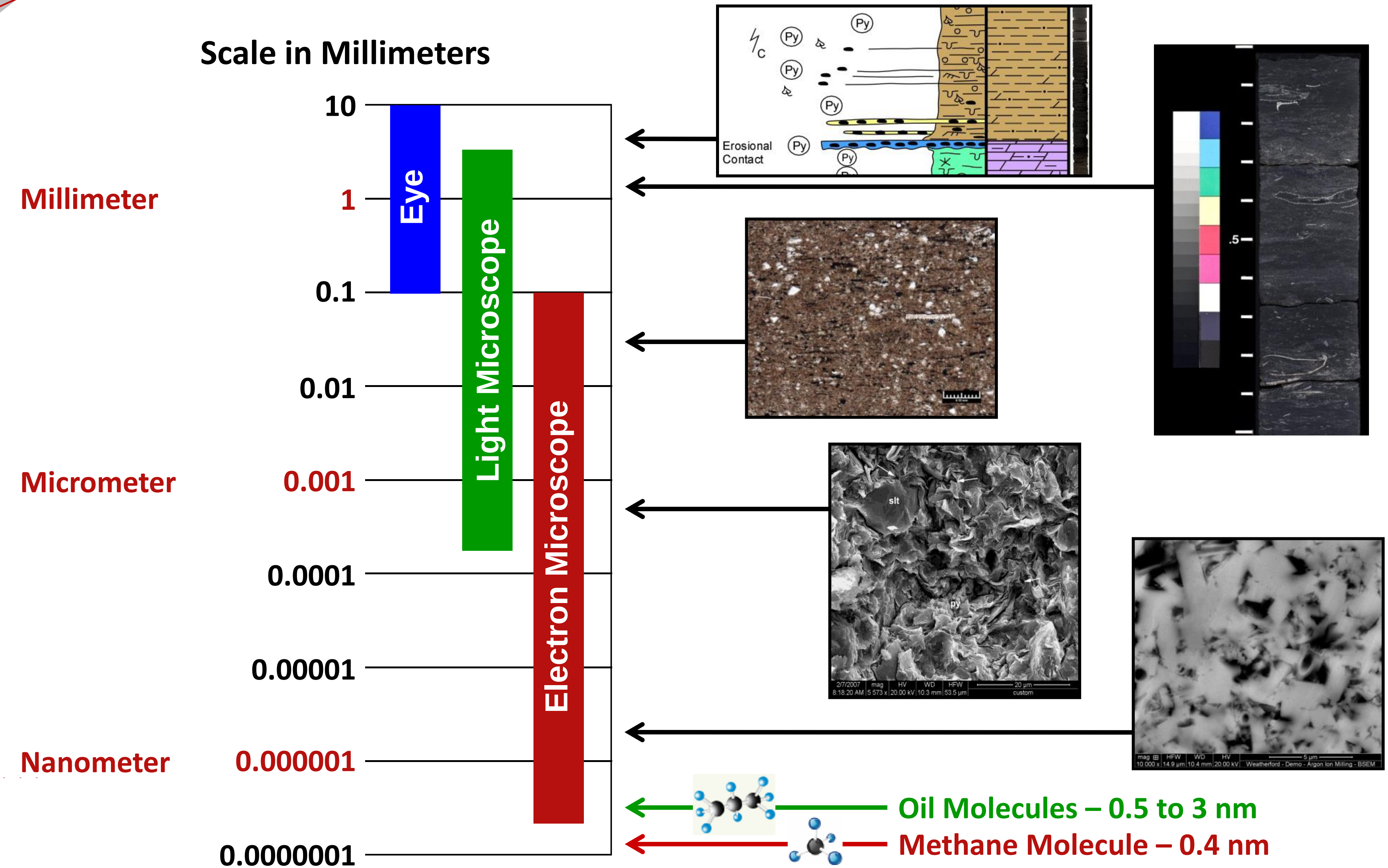

Pencillated Gilsonite

Pencillated Gilsonite

20X Air Objective

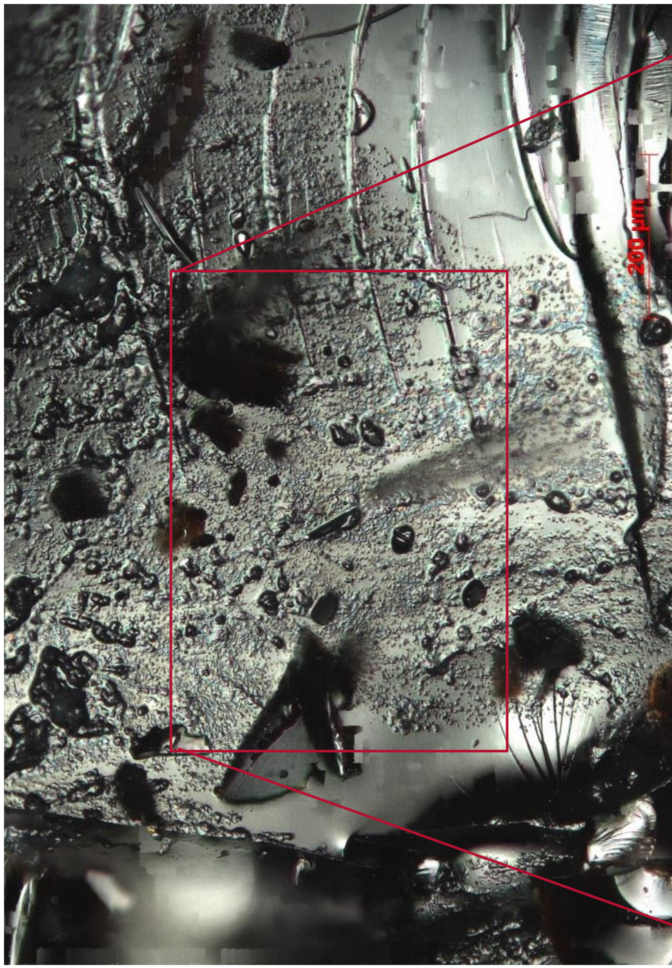

40X Air Objective

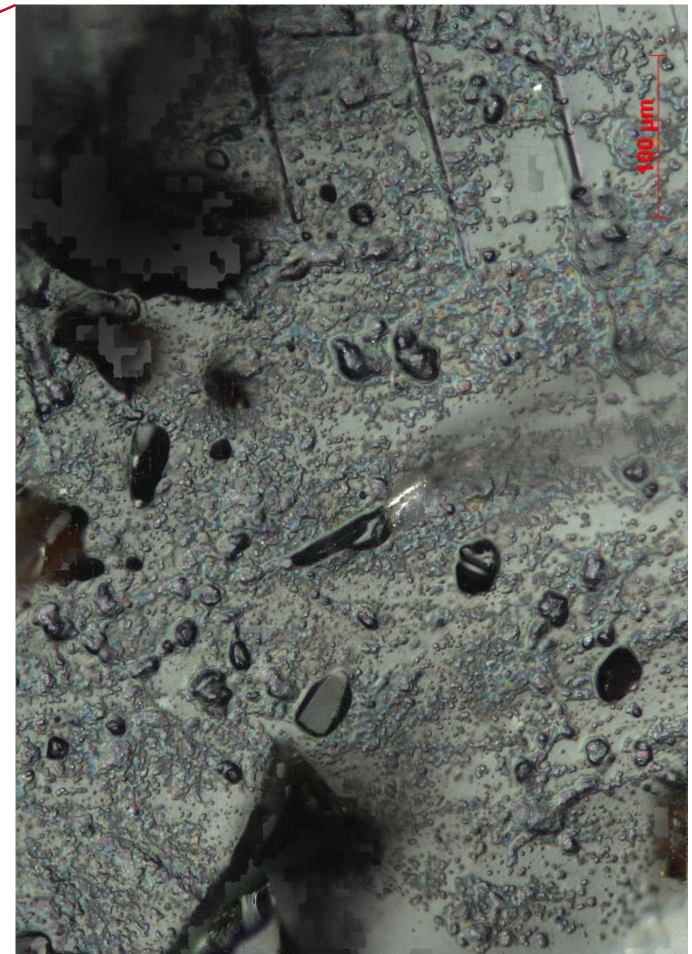

Micropore to mesopore size pitting evident

Weatherford®
LABORATORIES

Pencillated Gilsonite

40X Air Objective

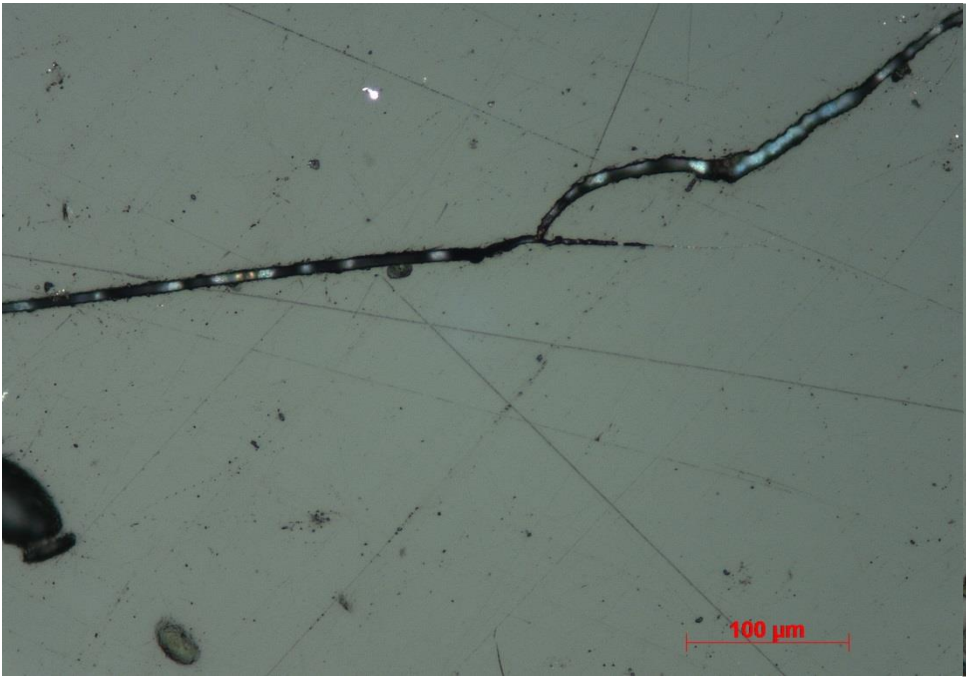

Typical field of view of ‘pencillated’ plane using 40x air objective.

40X Air Objective

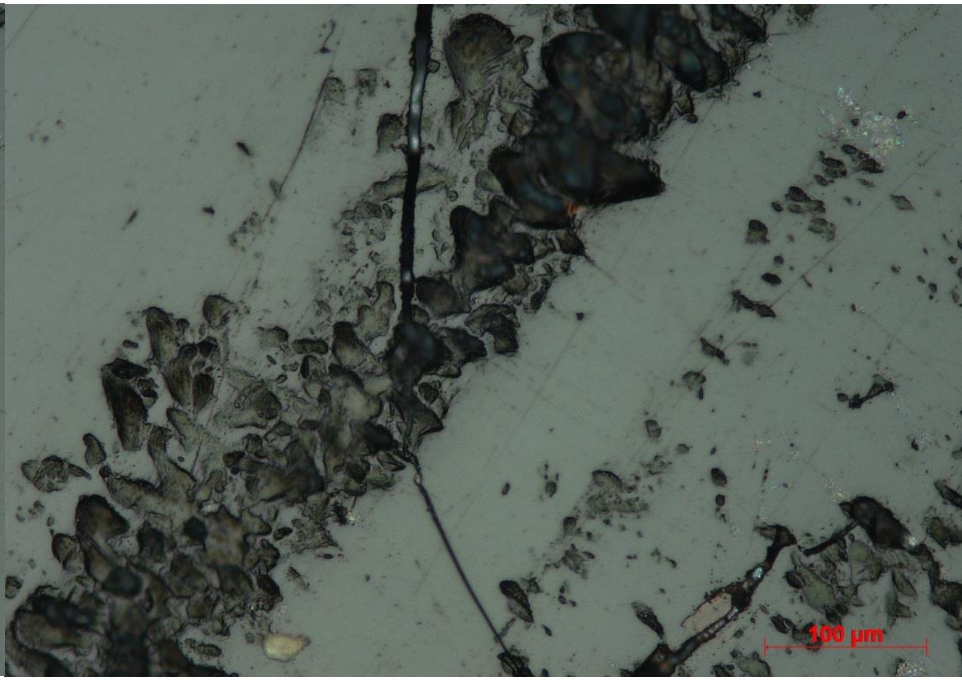

Additional photomicrograph showing less common pitted pattern not attributed to polishing process.

Weatherford®
LABORATORIES

Pencillated Gilsonite

80X SEM

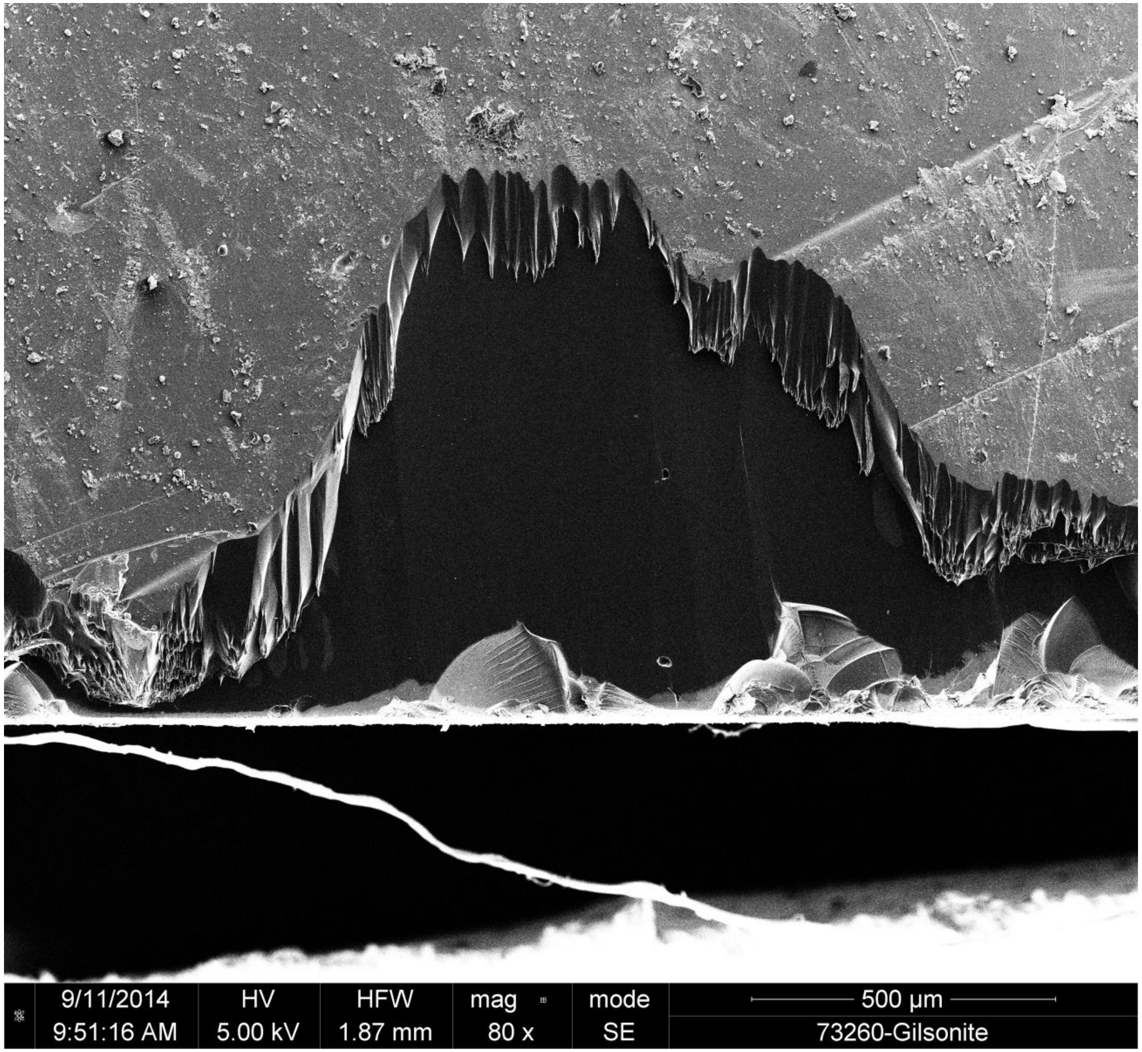

Ion milled surface exhibits no nanoporosity with rare micropore pits

Weatherford LABORATORIES

Pencillated Gilsonite

1550X SEM

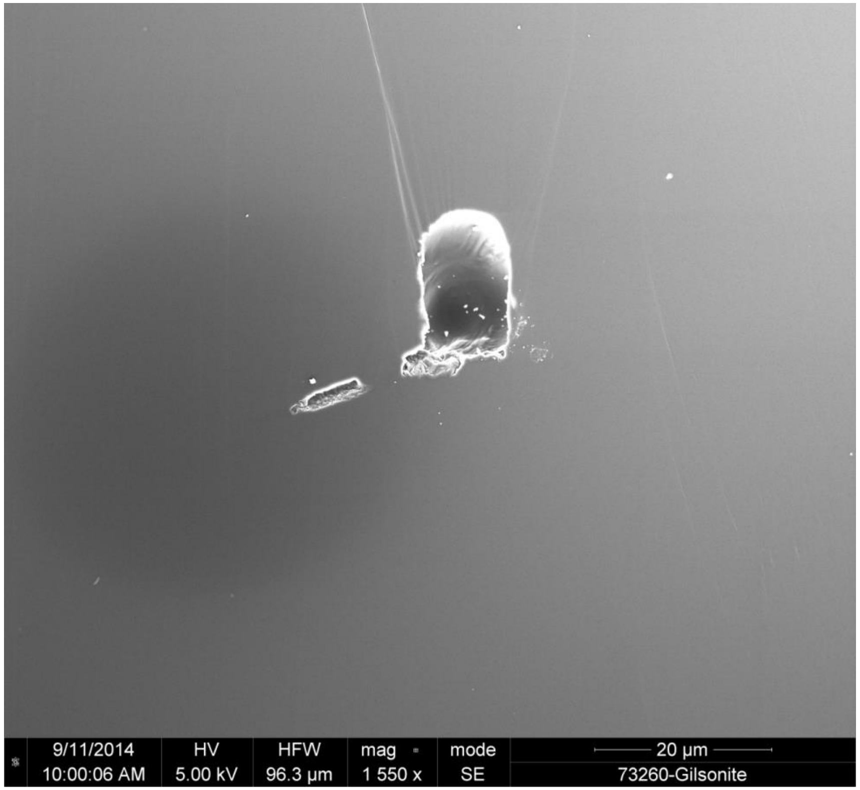

Matrix is featureless and rare micropore pits are discontinuous

5000X SEM

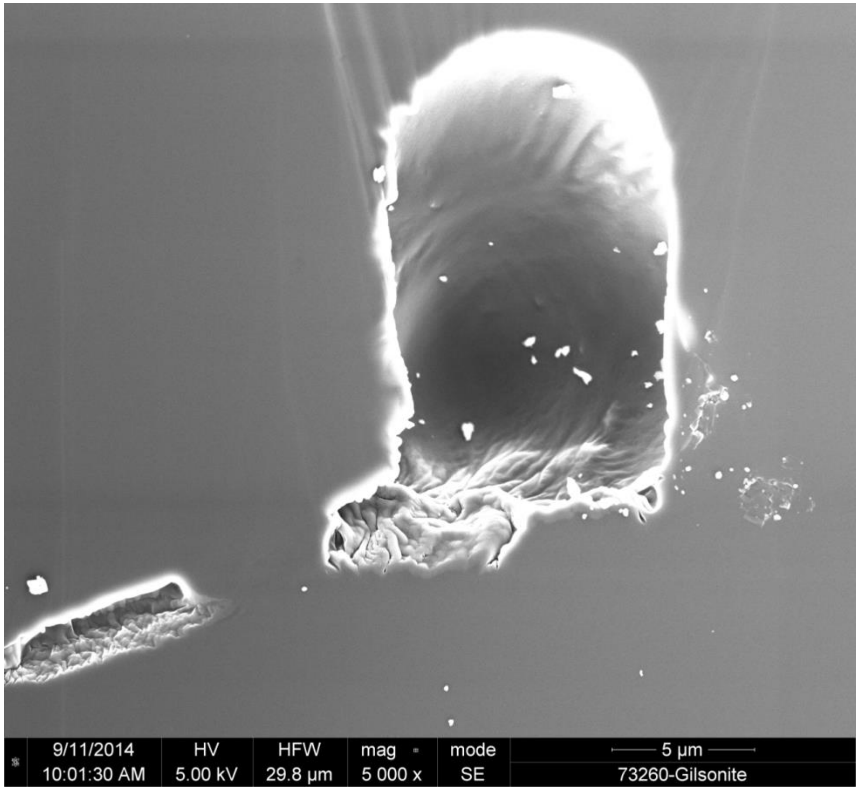

Enlarged view of discontinuous micropore pits

Weatherford® LABORATORIES

Pencillated Gilsonite

500X SEM

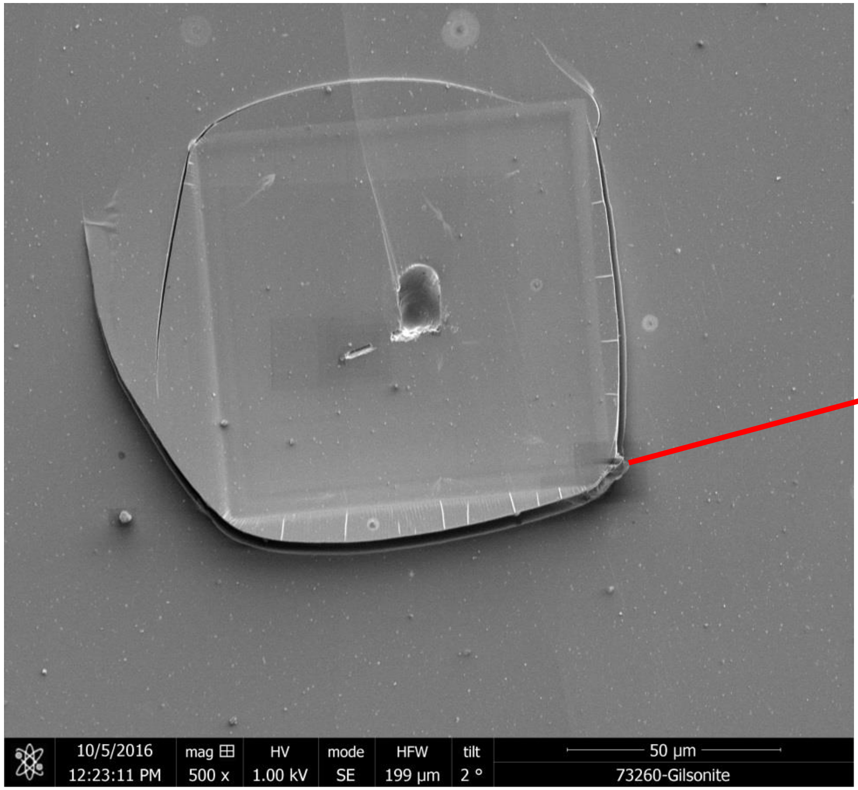

Matrix exhibits alteration associated with SEM imaging upon re-examination

6000X SEM

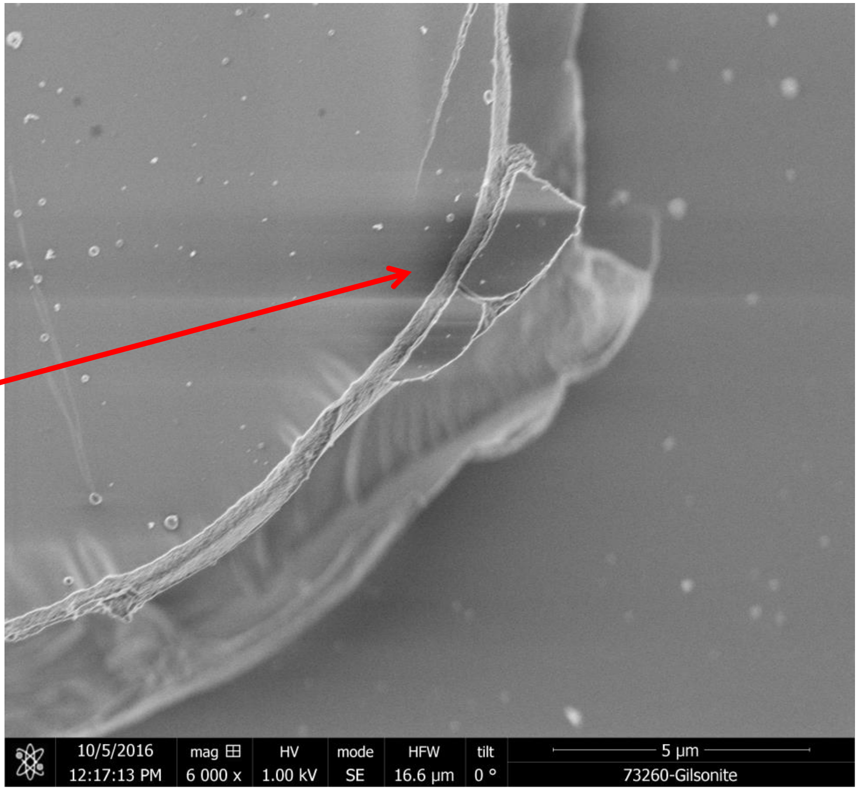

Observed SEM induced fractures and distortion within matrix

Weatherford®
LABORATORIES

Pencillated Gilsonite

85000X SEM

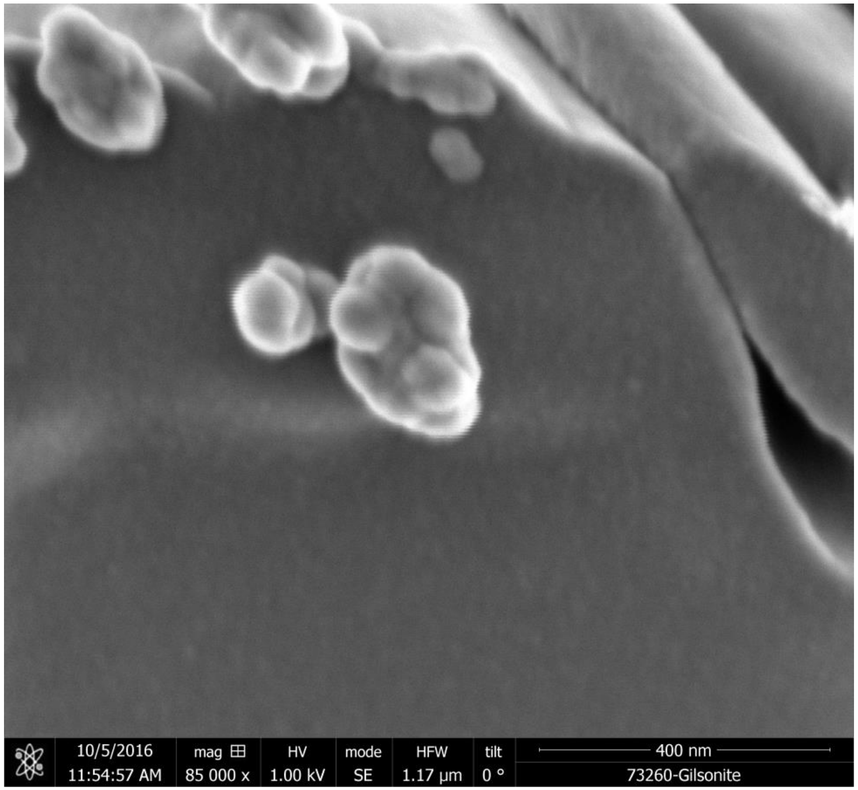

No occurrence of organic porosity even at high magnification

100000X SEM

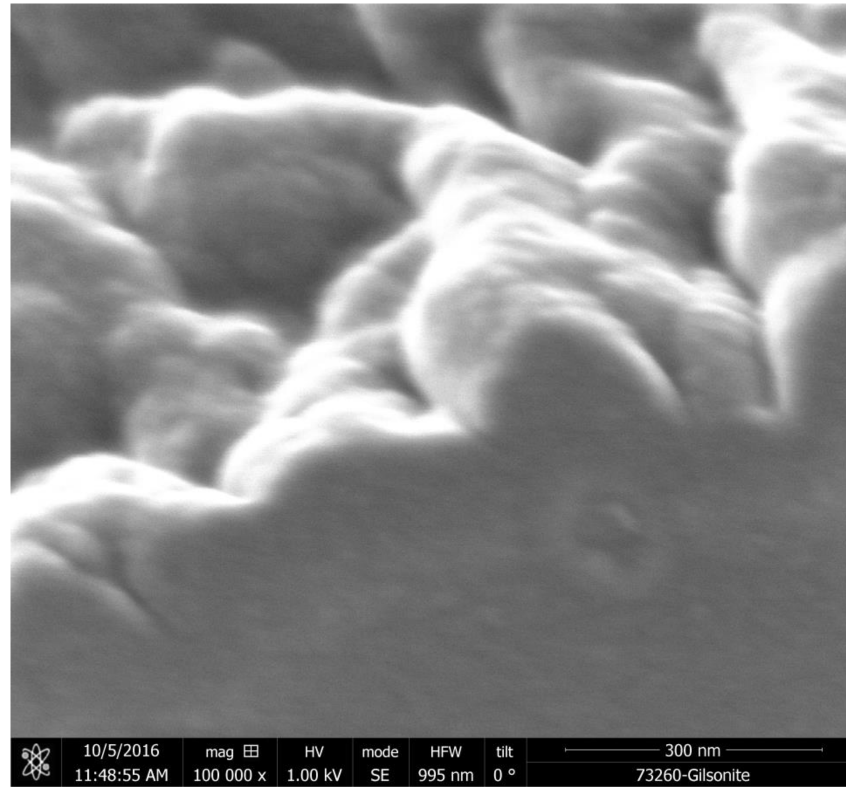

Subtle textural features do not appear to be associated with organic porosity

Weatherford® LABORATORIES

Pencillated Gilsonite

Better…Stronger…Faster
Bobby Hooghan is the Million Magnification Man

1000000X SEM

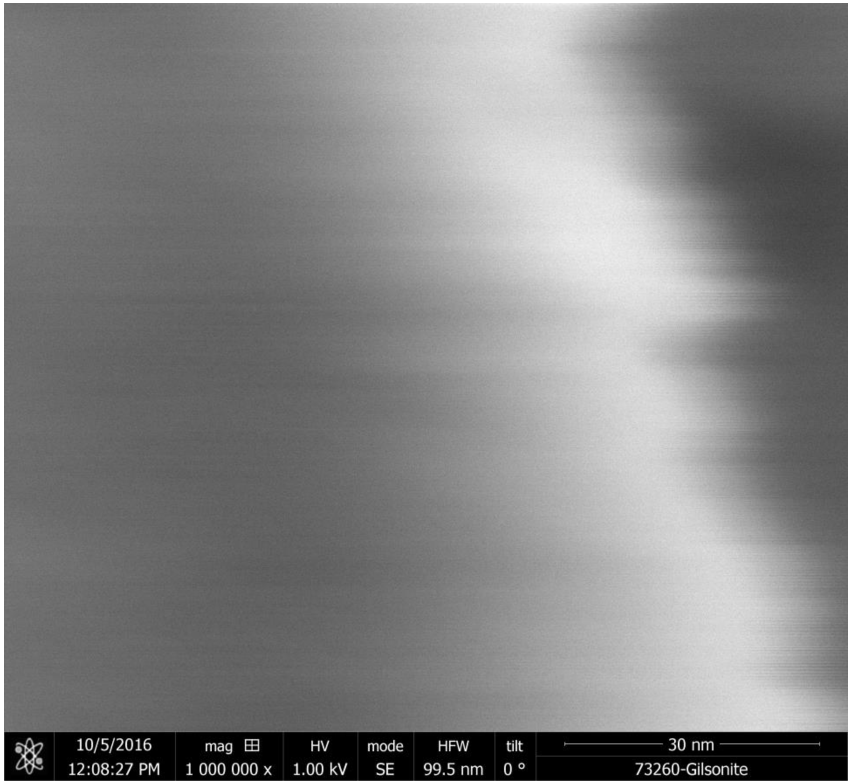

Still no visible organic porosity

Pencillated Gilsonite

5000X SEM SE

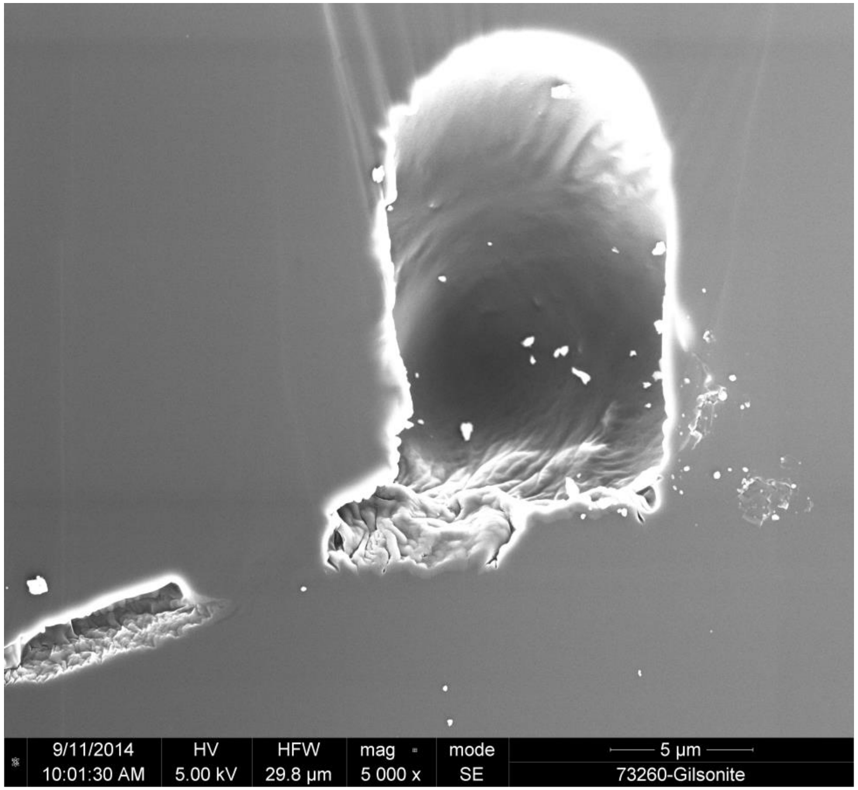

5000X SEM BSE

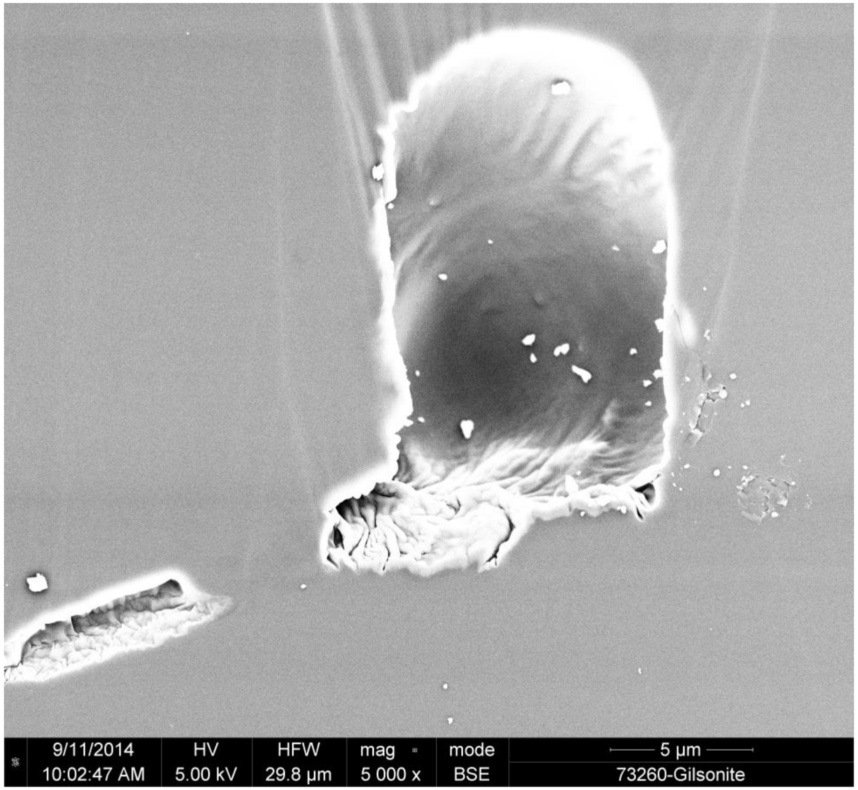

No major difference between secondary electron image and backscatter image…..still no evident porosity

Weatherford® LABORATORIES

Conchoidal Gilsonite

10X Air Objective

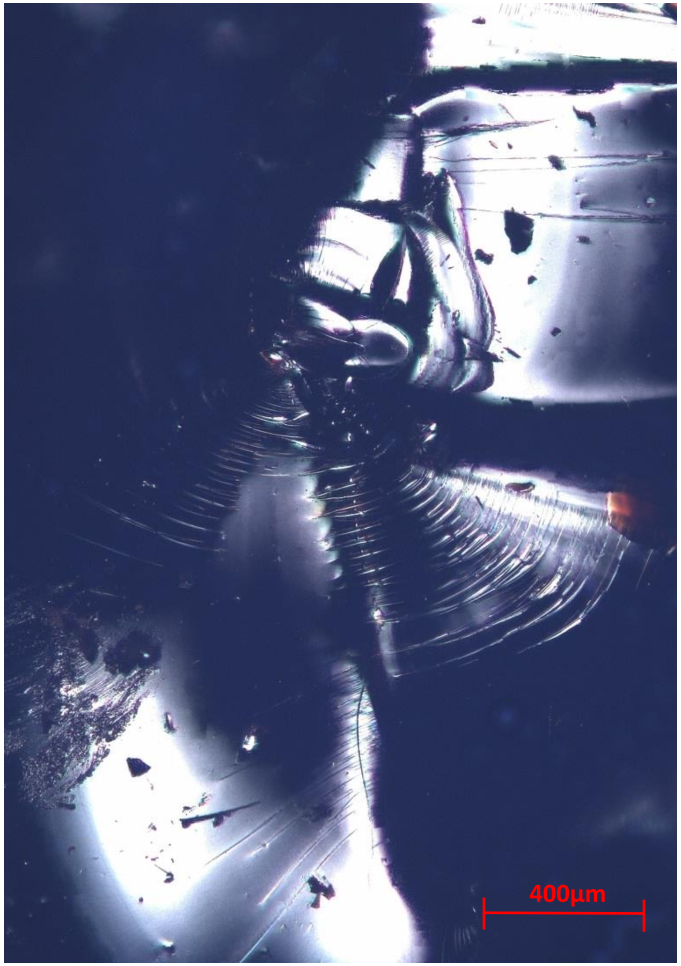

Weatherford®
LABORATORIES

Conchoidal Gilsonite

20X Air Objective

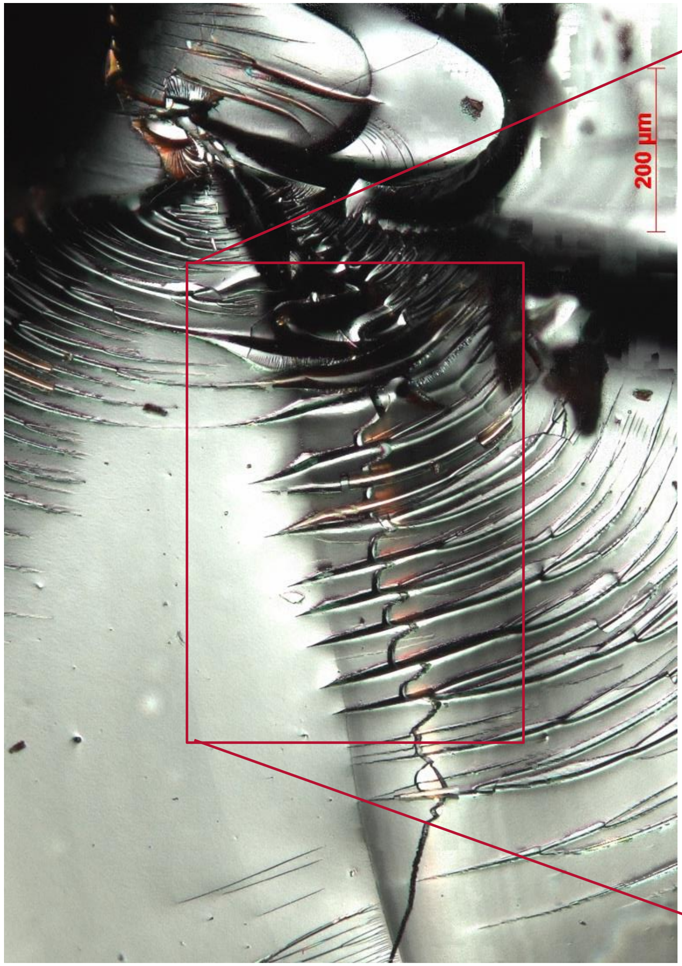

40X Air Objective

Typical twist hackle mark created by breaking sample

Weatherford® LABORATORIES

Joints and Shear Fractures

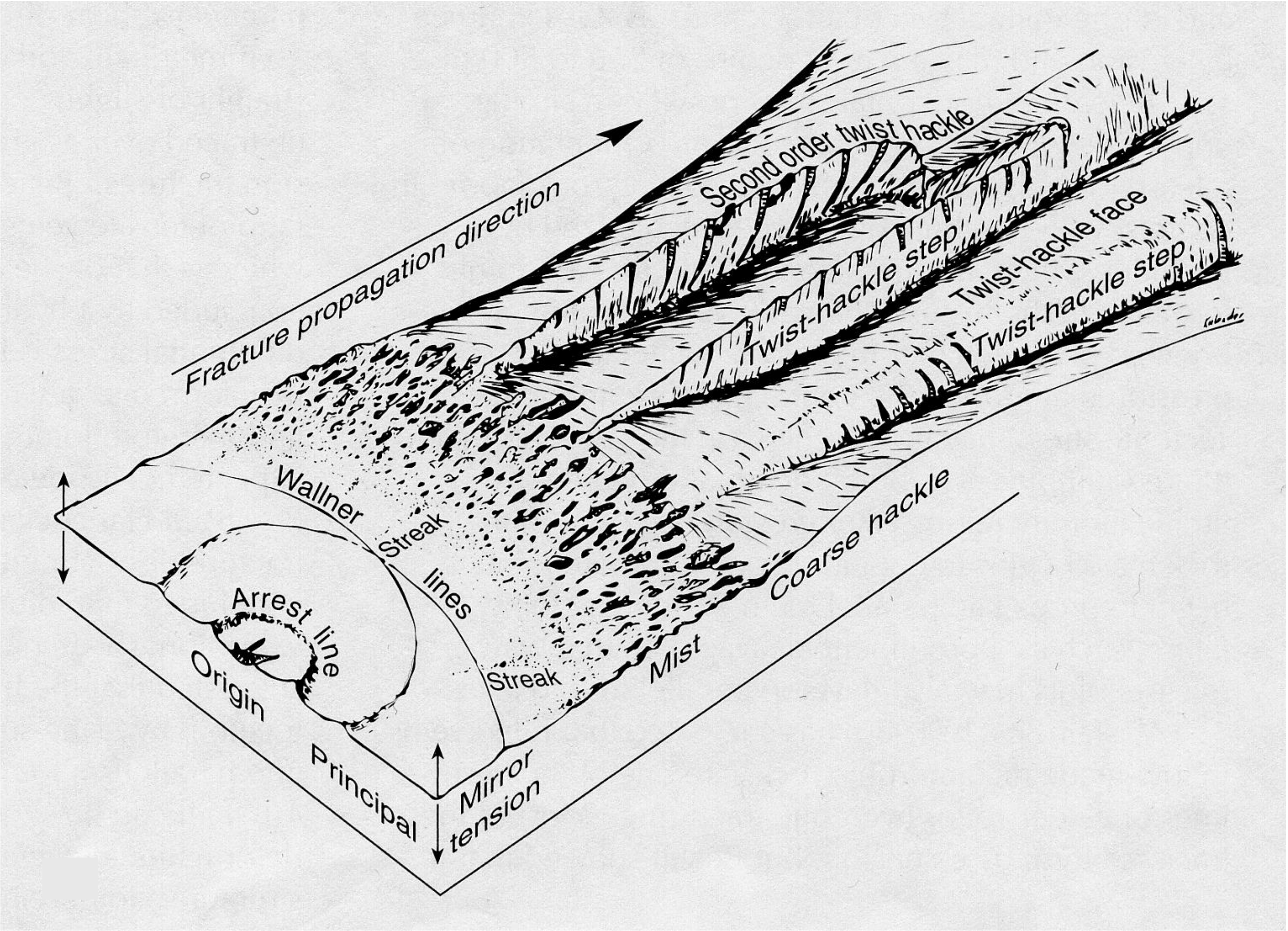

from Jim Speer http://isu.indstate.edu/jspeer/Structure/

Weatherford LABORATORIES

Conchoidal Gilsonite

1000X SEM

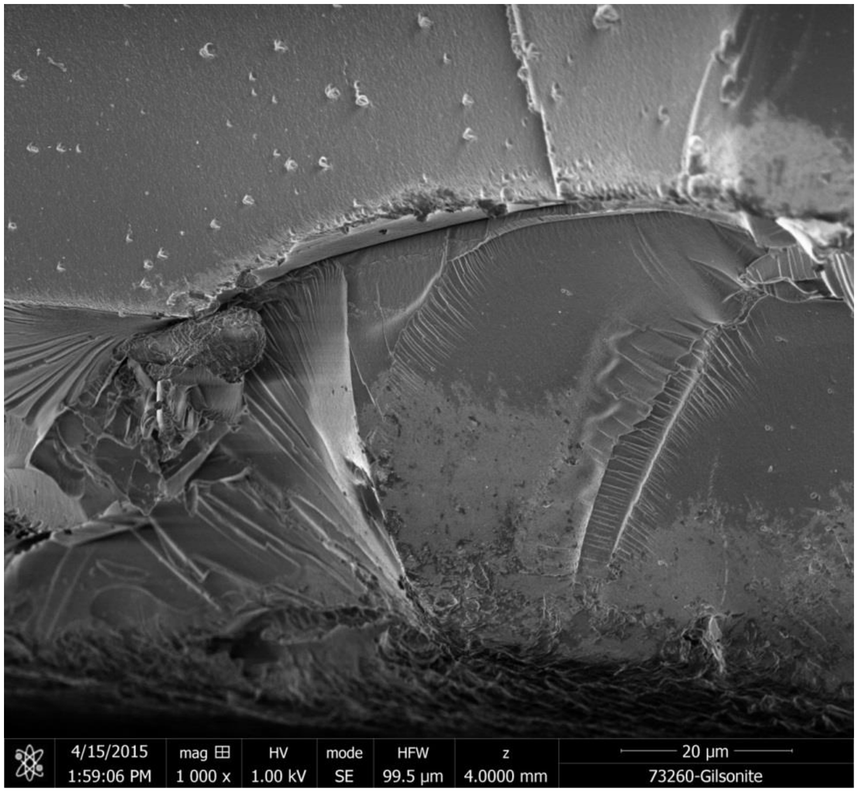

Conchoidal fractures evident but matrix shows no organic porosity

3500X SEM

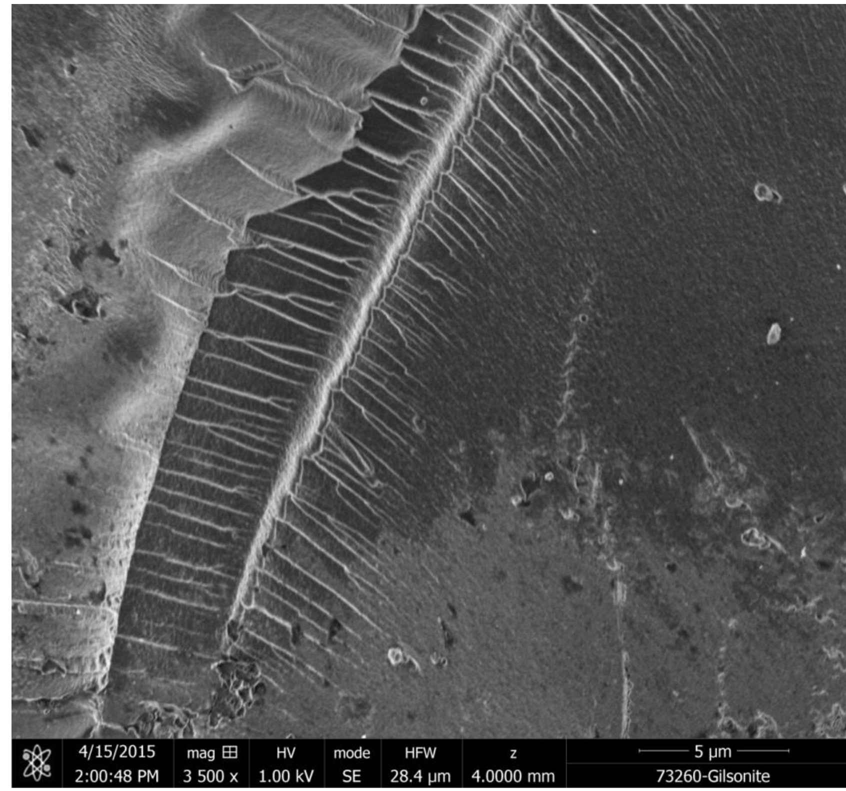

Fracture plane with twist hackle marks

Weatherford®
LABORATORIES

Conchoidal Gilsonite

250X SEM

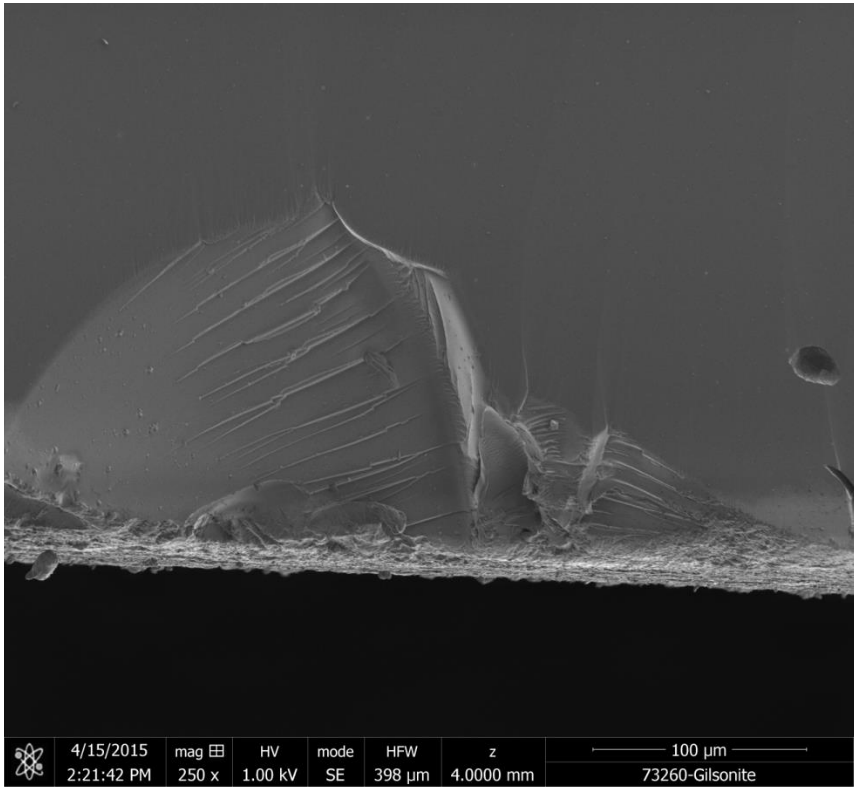

Edge of conchoidal fracture surface

2500X SEM

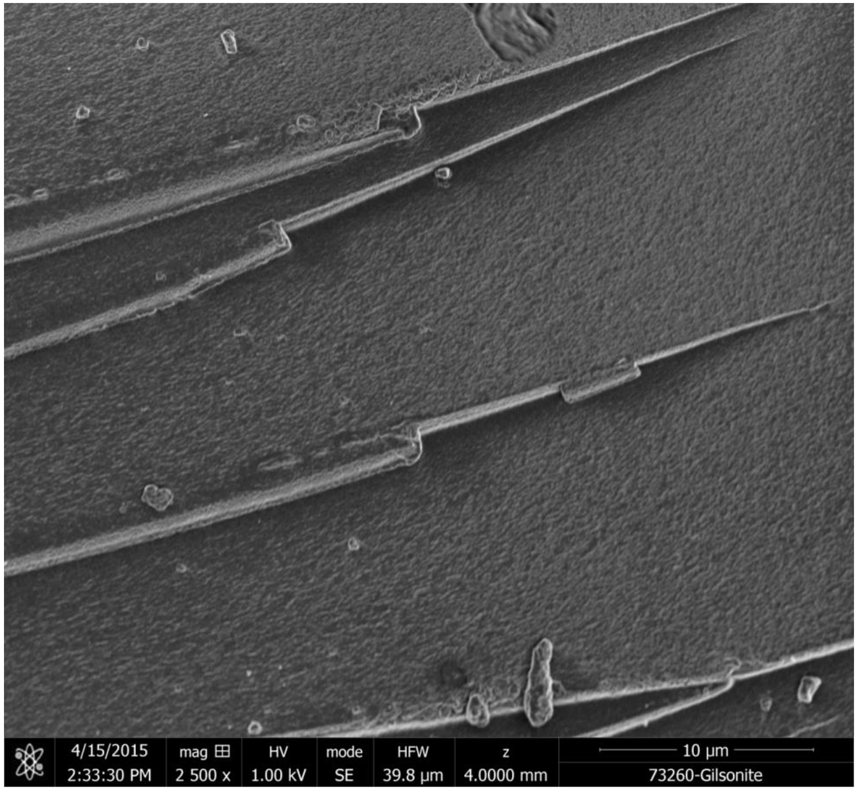

Enlarged twist hackle marks

Weatherford® LABORATORIES

Conchoidal Gilsonite under Oil Immersion

80X Oil Immersion Objective

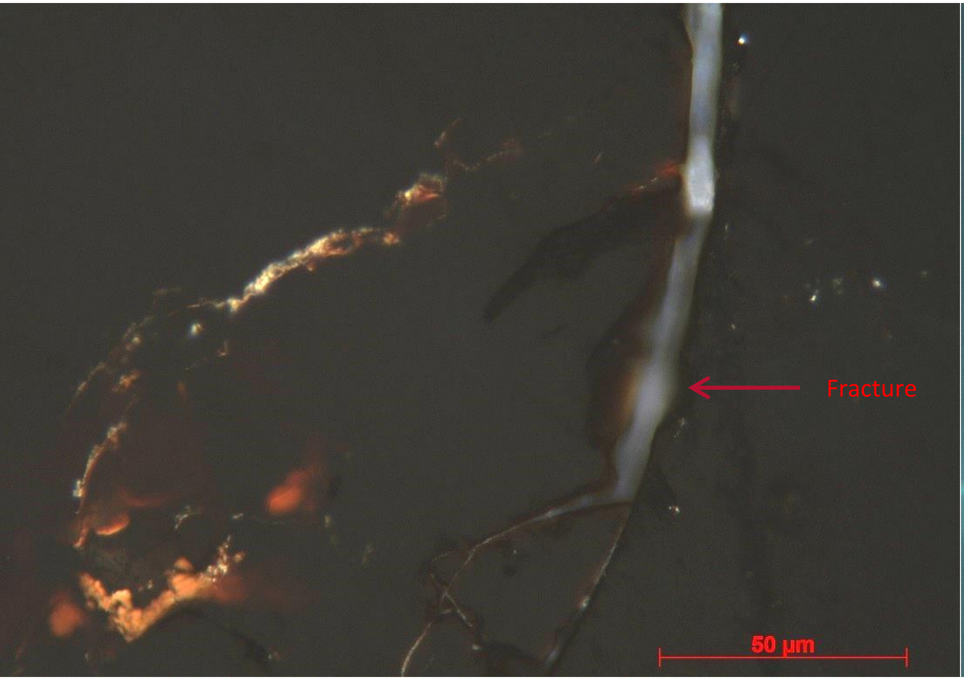

Reflected white light photomicrograph of conchoidal fracture plane. Note translucent brown area to left typical of bitumens.

80X Oil Immersion Objective

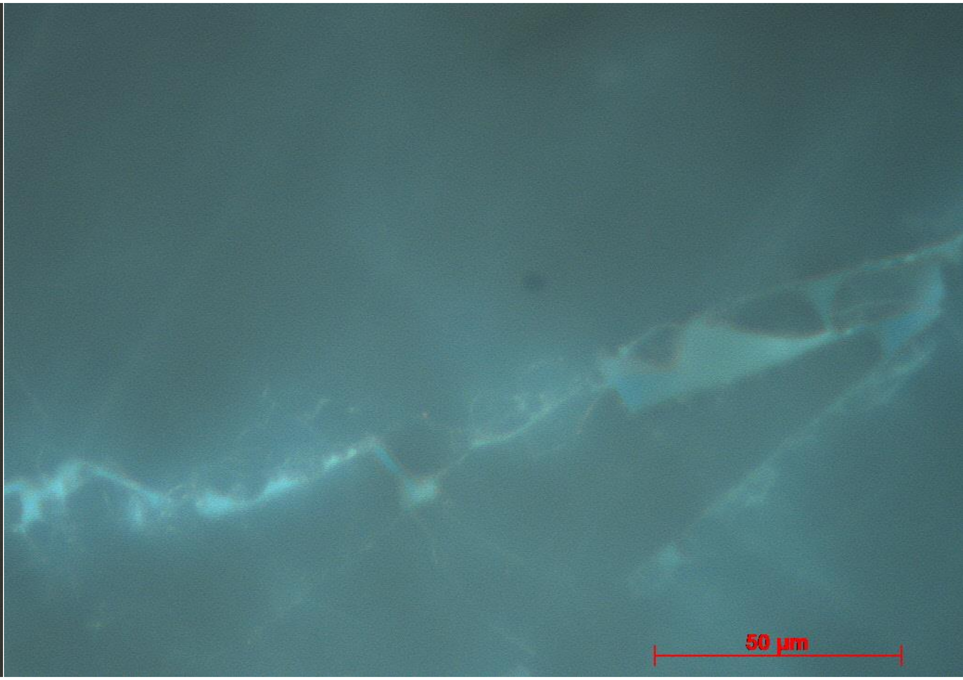

Reflected UV photomicrograph of fracture in conchoidal plane showing a 'fog' of mobile hydrocarbons leeching from fracture.

Weatherford LABORATORIES

Gilsonite Tilted View Imaging

90°/150X SEM

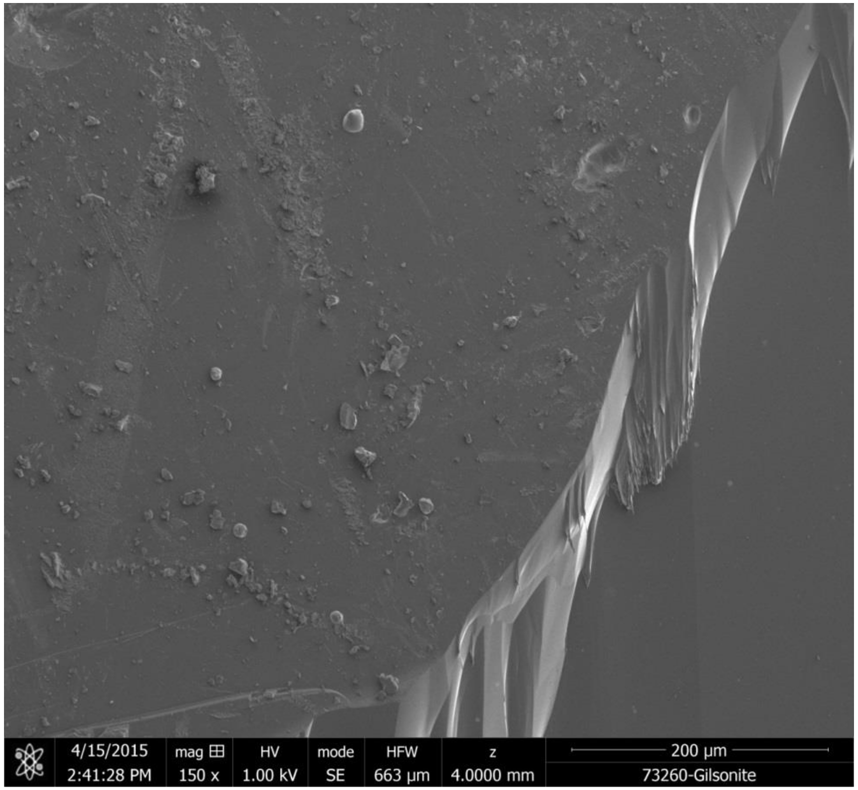

Ion milled contact – perpendicular view

45°/200X SEM

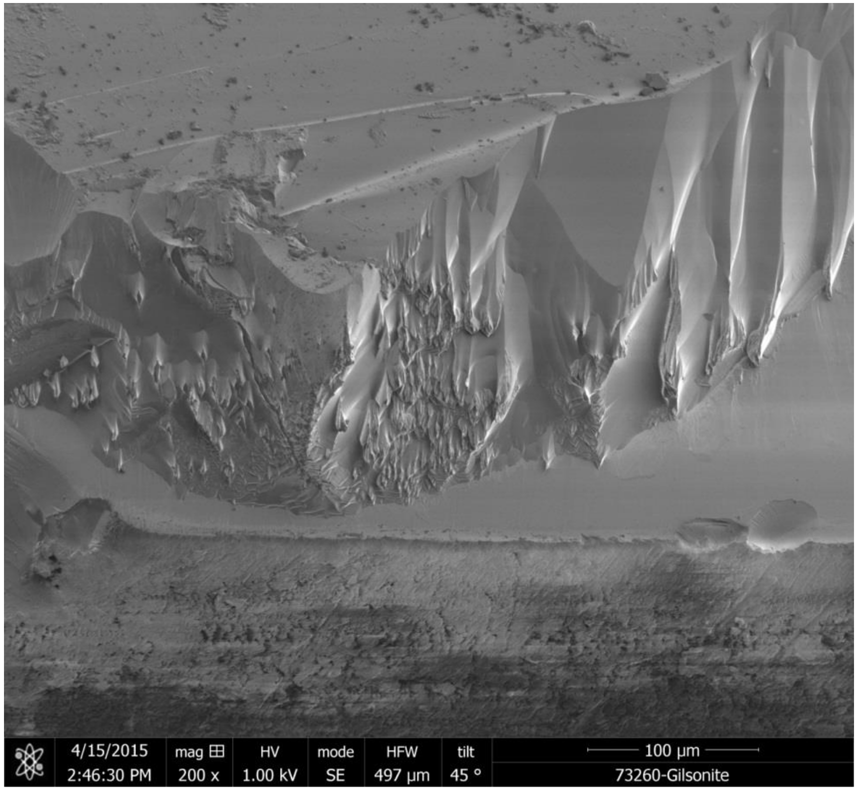

Ion milled contact – tilted view

Weatherford® LABORATORIES

Gilsonite Tilted View Imaging

45°/800X SEM

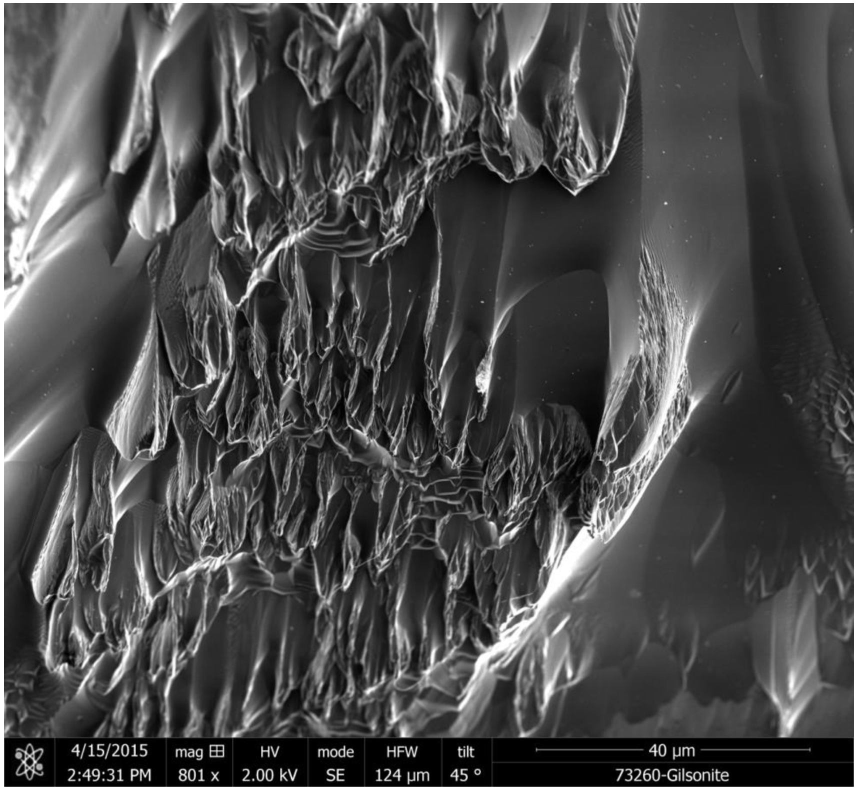

Conchoidal fracture surfaces in enlarged ion milled contact – tilted view

45°/800X SEM

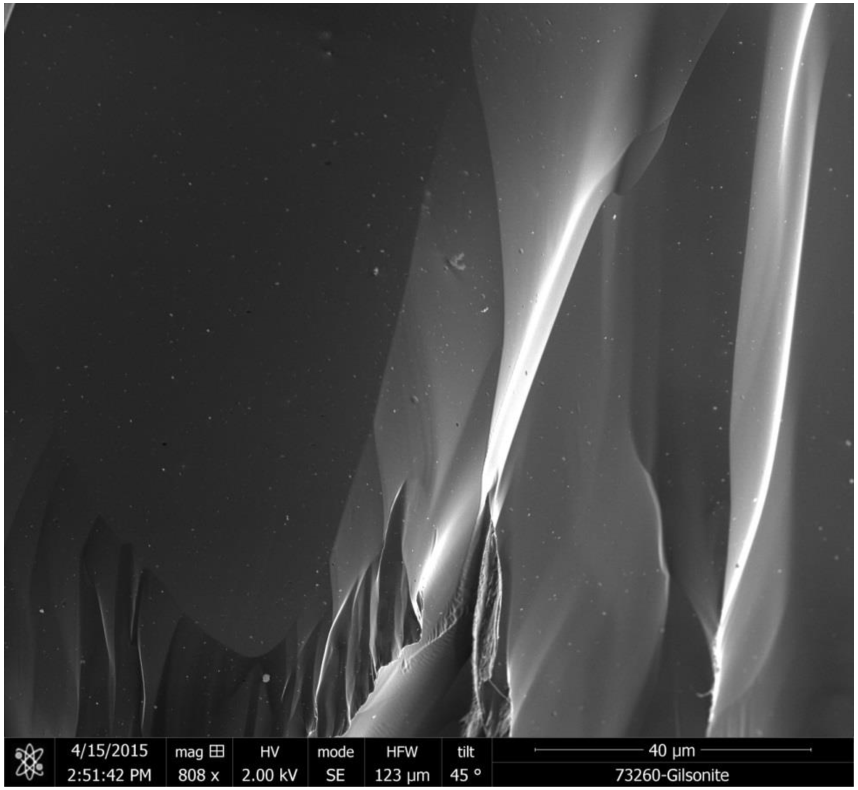

Absence of nanoporosity in enlarged ion milled contact – tilted view

Weatherford® LABORATORIES

Organic Petrology & SEM Observations

- Polished surfaces are typically dark grey and featureless. Macerals and inorganics are absent.
- Visual estimates suggest that fractures make up approximately 1% of the conchoidal fracture plane.
- Visual estimates of the pencillated plane suggest approximately 2% of the surface contains fractures but also 5% shallow pits.
- SEM imaging at all scales and angles confirms morphology of fractures and pitting along with the absence of organic porosity in gilsonite.

Weatherford® LABORATORIES

Summary Thoughts

- Unlike pyrobitumen, pre-oil solid bitumen represented by gilsonite was found to contain no significant organic nanoporosity in its matrix.
- Gilsonite does have minor pitting and fractures, but these do not represent an effective interconnected pore network and are probably artifacts of weathering/sampling.
- Bitumen and oil are thought to represent two different immiscible phases when water is present, especially water dissolved in the liquid bitumen phase.
- Depending upon thermal maturity, unconventional source rock reservoirs may contain bitumen, oil or both, which form a continuous expulsion/migration pathway.

Weatherford® LABORATORIES

References

- Boden, T. and Tripp, B.T., 2012, *Gilsonite veins of the Uinta Basin, Utah*, Utah Geological Survey, Special Study 141, CD-ROM publication, 50 p., 1 pl.
- Curiale, J.A., 1986, Origin of solid bitumens, with emphasis on biological marker results, in Leythaeuser, D. and Rullkötter, J., eds., Advances in Organic Geochemistry 1985, Pergamon Press, New York, p. 559-580.
- Eldridge, G.H., 1901, The asphalt and bituminous rock deposits of the United States, in 22nd Annual Report of the U.S. Geological Survey, 1900-1901, Government Printing Office, Washington D.C., v. 22, pt. 1, p. 209-452.
- Helms, J.R., Kong, X., Salmon, E., Hatcher, P.G., Schmidt-Rohr, K., and Mao, J., 2012, Structural characterization of gilsonite bitumen by advanced nuclear magnetic resonance spectroscopy and ultrahigh resolution mass spectrometry revealing pyrrolic and aromatic rings substituted with aliphatic chains, Organic Geochemistry, v. 44, p. 21-36.
- Hunt, J.M., 1963, Composition and origin of the Uinta Basin bitumens, in Crawford, A.L., ed., Oil and Gas Possibilities of Utah, Re-evaluated, Utah Geological and Mineralogical Survey, Bulletin 54, paper 24, Utah Geological Society, Salt Lake City, p. 249-273.
- Hunt, J.M., 1979, *Petroleum geochemistry and geology*, W. H. Freeman and Company, San Francisco, 617 p.
- Lewan, M.D., 1987, Petrographic study of primary petroleum migration in the Woodford Shale and related rock units, in Doligez, B., ed., Migration of Hydrocarbons in Sedimentary Basins, Editions Technip, Paris, p. 113-130.
- Lewan, M.D., 2011, Petroleum formation research through hydrous pyrolysis, Weatherford Laboratories Presentation, June 17, 2011.
- Ruble, T.E., Lewan, M.D., and Philp, R.P., 2001, New insights on the Green River petroleum system in the Uinta basin from hydrous pyrolysis experiments, AAPG Bulletin, v. 85, n. 8, p. 1333-1371.

Weatherford®
LABORATORIES